공학박사 학위논문

New PTS Schemes Using Reduced-Complexity Generation of Alternative OFDM Signal Vectors

저복잡도 후보 OFDM 신호 생성을 이용한 새로운 PTS 방법

2014년 2월

서울대학교 대학원

전기·정보공학부

조 영 전

New PTS Schemes Using Reduced-Complexity Generation of Alternative OFDM Signal Vectors

지도 교수 노종선

이 논문을 공학박사 학위논문으로 제출함.

2013년 11월

서울대학교 대학원

전기·정보공학부

조 영 전

조영전의 공학박사 학위논문을 인준함.

2013년 12월

위 원 장 _____ (인)

부위원장 _____ (인)

위 원 _____ (인)

위 원 _____ (인)

위 원 _____ (인)

New PTS Schemes Using Reduced-Complexity Generation of Alternative OFDM Signal Vectors

Presented to the Graduate School of Seoul National University in Partial Fulfillment of the Requirements for

THE DEGREE OF DOCTOR OF PHILOSOPHY

by

Young-Jeon Cho

Department of Electrical and Computer Engineering

Seoul National University

This dissertation approved for

THE DEGREE OF DOCTOR OF PHILOSOPHY

December, 2013

Chairman _____

Vice Chairman _____

Member _____

Member _____

Member _____

Abstract

New PTS Schemes Using Reduced-Complexity Generation of Alternative OFDM Signal Vectors

Young-Jeon Cho
Department of ECE
The Graduate School
Seoul National University

This dissertation proposes several research results on the peak-to-average power ratio (PAPR) reduction schemes for the orthogonal frequency division multiplexing (OFDM) systems. The PAPR is the one of major drawback of OFDM system which causes signal distortion when OFDM signal passes through nonlinear high power amplifier (HPA). Various schemes have been proposed to reduce the PAPR of OFDM signals such as clipping, selected mapping (SLM), partial transmit sequence (PTS), active constellation extension (ACE), companding, and tone reservation (TR). Among them, PTS scheme can transmit an OFDM signal vector by generating many alternative OFDM signal vectors using the partitioned subblock signals and selecting the optimal OFDM signal vector with the minimum PAPR. However, the PTS scheme requires large computational complexity, because it needs many inverse fast Fourier transforms (IFFTs) of subblock signals and lots of alternative OFDM signal vectors are generated. In this dissertation, we concentrate on reducing the computational complexity of the PTS scheme.

In the first part of this dissertation, we propose a new PTS scheme with low computational complexity using two search steps to find a subset of phase rotating vectors showing good PAPR reduction performance. In the first step, sequences with low correlation are used as phase rotating vectors for PTS scheme, which are called the initial phase vectors. Kasami sequence and quaternary sequence are used in this step as the initial phase vectors. In the second step, local search is performed based on the initial phase vectors to find additional phase rotating vectors which show good PAPR reduction performance. Numerical analysis shows that the proposed PTS scheme can achieve almost the same PAPR reduction performance as the conventional PTS scheme with much lower computational complexity than other low-complexity PTS schemes.

In the second part of the dissertation, we propose another low-complexity PTS schemes using the dominant time-domain OFDM signal samples, which are only used to calculate PAPR of each alternative OFDM signal vector. In this PTS scheme, we propose efficient metrics to select the dominant time-domain samples. For further lowering the computational complexity, dominant time-domain samples are sorted in decreasing order by the proposed metric values and then the power of each sample is compared with the minimum PAPR of the previously examined alternative OFDM signal vectors. Numerical results confirm that the proposed PTS schemes using new metrics show large computational complexity reduction compared to other existing low-complexity PTS schemes without PAPR degradation.

In the last part of the dissertation, for the reduced-complexity PTS scheme, a new selection method of the dominant time-domain samples is proposed by rotating the IFFTed signal samples to the area on which the IFFTed signal sample of the first subblock is located in the signal space. Moreover, the method of pre-exclusion of the phase rotating vectors using the time-domain sample rotation is proposed to reduce the number of alternative OFDM signal vectors. Further, three proposed PTS schemes are introduced to reduce the computational complexity by using simple OFDM signal rotation and pre-exclusion of the phase rotating vectors. Numerical analysis shows that the proposed PTS schemes achieve the same PAPR reduction performance as that of the conventional PTS scheme with the large computational complexity reduction.

Keywords: Fast Fourier transform (FFT), inverse fast Fourier transform (IFFT), Kasami sequences, orthogonal frequency division multiplexing (OFDM), partial transmit sequence (PTS), peak-to-average power ratio (PAPR), phase rotating vector, quaternary sequences.

Student ID: 2010-30801

Contents

List of Tables

List of Figures

Chapter 1. Introduction

1.1. Background

The idea of orthogonal frequency-division multiplexing (OFDM) has been proposed since the 1950s. It has been used from at least the 1960s as multicarrier modulation opposed to the single-carrier modulation, but OFDM is hard to implement with the electronic hardware at that time [1]. Thus, it does not have been used in commercial communication systems due to its high cost for hundreds of oscillators. In the 1990s, the OFDM has experienced a breakthrough with developments of digital signal processing technology. Due to its bandwidth efficiency and robustness against frequency selective fading, OFDM has been widely used in modern wireless communications.

With rapid development of wireless communication theory and hardware technologies, OFDM has been adopted in many wireless communication systems [2], for example, the digital audio broadcasting (DAB), the digital video broadcasting (DVB), IEEE 802.11a/g/n standards, long-term evolution (LTE), ultra-wideband (UWB), wideband wireless metropolitan-area network (MAN), WiMAX, etc.

OFDM has many advantages such as high data transmission rate and robustness against intersymbol interference (ISI) and fading from multi-path propagation. However, the OFDM signal is basically a sum of N

complex random variables, each of which can be considered as a complex modulated signal at different frequencies. Thus, all the signal components may add up in phase and produce a large output causing large peak-to-average power ratio (PAPR), which degrades the efficiency of nonlinear high power amplifier (HPA) [3]. The main purpose of this dissertation is to reduce the PAPR of OFDM signals.

In order to alleviate the PAPR problem of OFDM signals, many PAPR reduction schemes have been proposed. Clipping is the simplest scheme to reduce PAPR, but it gives rise to regrowth of peak and increases bit error rate (BER) [4]. The tone reservation (TR) reserves some tones for generating a PAPR reduced OFDM signal vector [5]. However, these reserved tones are not used for data transmission, which causes data rate loss. The selected mapping (SLM) [6] and partial transmit sequence (PTS) [7] generate alternative OFDM signal vectors and then select the alternative OFDM signal vector with the minimum PAPR, but they requires side information and many inverse fast Fourier transforms (IFFTs). Also, there are many PAPR reduction schemes such as active constellation extension (ACE) [8] and companding [9][10]. None of them are perfect solution, which increases power, BER, data rate loss, and computational complexity.

Modified PTS schemes are proposed to reduce computational complexity of the conventional PTS scheme. Particularly, when the number of IFFTs is fixed, generation and PAPR comparison of alternative OFDM signal vectors are mainly considered to alleviate the computational com-

plexity.

1.2. Overview of Dissertation

Chapter 2 explains OFDM system model, characteristic of nonlinear HPA, and the definition of PAPR. Also, two type of HPA and several different methods to define the ratio of the peak power to the mean power are explained. Further, some analytical methods to derive the complementary cumulative distribution function (CCDF) of PAPR are explained.

In Chapter 3, the well-known PAPR reduction schemes are explained, which include clipping, SLM, and PTS. Since this dissertation focus on low-complexity PTS, some existing low-complexity PTS schemes are also reviewed.

In Chapter 4, a new PTS scheme with low computational complexity is proposed, where two search steps are taken to find a subset of phase rotating vectors showing good PAPR reduction performance. In the first step, sequences with low correlation are used as phase rotating vectors for PTS scheme, which are called the initial phase vectors. In the second step, local search is proposed based on the initial phase vectors to find additional phase rotating vectors which show good PAPR reduction performance.

In Chapter 5, another low-complexity PTS schemes are proposed, where the PAPR values of alternative OFDM signal vectors are approximately computed based on the dominant time-domain samples selected by using a simple power metric. Here, two new effective metrics for select-

ing dominant time-domain samples are proposed for the low-complexity PTS scheme. For further lowering the computational complexity, two low-complexity PTS schemes are proposed by sorting the dominant time-domain samples in decreasing order by their metric values. Simulation results confirm that the proposed PTS schemes show identical PAPR reduction performance with substantially reduced computational complexity, compared to the conventional PTS scheme.

In Chapter 6, a new selection method of the dominant time-domain samples are proposed by rotating the IFFTed signal samples to the area on which the IFFTed signal sample of the first subblock is located on the signal space. Moreover, the method of pre-exclusion of the phase rotating vectors using the time-domain sample rotation is proposed to reduce the number of alternative OFDM signal vectors. Further, three proposed PTS schemes are introduced to reduce the computational complexity by using simple OFDM signal rotation and pre-exclusion of the phase rotating vectors. Numerical results confirm that the proposed PTS schemes show large computational complexity reduction without PAPR degradation.

Finally, some concluding remarks are given in Chapter 7.

Chapter 2. PAPR in OFDM System

OFDM becomes an essential modulation technique in modern wireless communication systems due to its bandwidth efficiency and robustness to the multipath fading. However, PAPR of OFDM signals causes signal distortion due to the nonlinear effect of HPA, which causes in-band distortion, out-of-band radiation, and BER degradation at the receiver. In this chapter, an analytical model of OFDM system is described. Also, the input-output characteristic of HPA and basic concept of PAPR are explained.

2.1. OFDM System Model

Fig. 2.1 shows the typical OFDM transmitter. Serial binary bits are modulated by constellation mapping. This mapping can be used by phase shift keying (PSK) or quadrature amplitude modulation (QAM). The input symbol vector is fed into a serial to parallel (S/P) conversion that forms a parallel symbol streams.

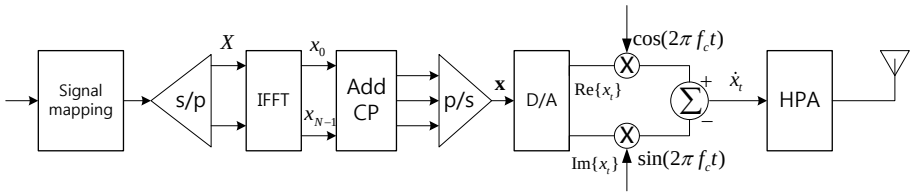

Figure 2.1: Block diagram of OFDM transmitter.

After serial to parallel conversion, an input symbol vector of length N can be represented as a vector $\mathbf{X} = [X_0, X_1, \cdots, X_{N-1}]^T$, where $X_k, k = 0, 1, \cdots, N-1$, are input symbols.

Taking IFFT operation on the input symbol vector, discrete baseband OFDM signal is expressed as

$$x_n = \frac{1}{\sqrt{N}} \sum_{k=0}^{N-1} X_k e^{j2\pi kn/N}, \ 0 \leq n \leq N-1 \tag{2.1}$$

where $\mathbf{x} = [x_0, x_1, \cdots, x_{N-1}]^T$ denotes the OFDM signal vector.

After that, cyclic prefix (CP) or guard interval of length N_g is appended to it. The CP helps in mitigating the effect of time delay by multipath fading, but it wastes bandwidth by using repeated symbols. The cyclically extended discrete complex OFDM signal is converted into a serial stream using parallel to serial (P/S) conversion. Then, the serial symbol stream passes through a digital-to-analog (D/A) converter to form the continuous baseband OFDM signal as

$$x_t = \frac{1}{\sqrt{N}} \sum_{k=0}^{N-1} X_k e^{j2\pi k\Delta ft}, \ 0 \leq t \leq T_u \tag{2.2}$$

where Δf is the frequency spacing between adjacent subchannels and T_u is OFDM symbol duration, that is, $\Delta f = 1/T_u$.

The continuous baseband OFDM signal is modulated using a carrier frequency for transmission through a wireless channel which is called a passband OFDM signal. The passband OFDM signal $\dot{x}_t$ is written as

$$\dot{x}_t = \mathrm{Re}\{x_t e^{j2\pi f_c t}\} \tag{2.3}$$

where $\mathrm{Re}\{\cdot\}$ is the real part of the complex signal and f_c is the carrier frequency. Finally, the passband OFDM signal goes through nonlinear HPA, which causes signal distortion due to the amplitude fluctuation of the OFDM signal.

2.2. Nonlinear High Power Amplifier Models

Amplitude fluctuation of OFDM signal is highly sensitive to the nonlinearity of HPA, which causes in-band distortion and out-of-band radiation of OFDM signals. Traveling wave tube amplifier (TWTA) and solid state power amplifier (SSPA) are well-known as two types of HPA. In order to approximate the amplitude modulation (AM) nonlinearity of TWTA and SSPA for the OFDM signals, simple mathematical models of AM distortion in TWTA and SSPA are explained.

An output of nonlinear HPA for a baseband OFDM signal $x_n = |x_n|e^{j\phi_n}$ is given as

$$y_n = G[|x_n|]e^{j(\phi_n + \Phi[|x_n|])} \tag{2.4}$$

where the functions $G[\cdot]$ and $\Phi[\cdot]$ denote the AM/AM and AM/PM conversion characteristics of the nonlinear amplifier, respectively. Based on (2.4), TWTA can be given as Saleh's model [11]

$$G[|x_n|] = \frac{\alpha_G|x_n|}{1+\beta_G|x_n|^2} \text{ and } \Phi|x_n| = \frac{\alpha_\Phi|x_n|^2}{1+\beta_\Phi|x_n|^2} \tag{2.5}$$

where α_G, β_G, α_Φ, and β_Φ determine the characteristics of TWTA.

In SSPA models, Rapp model and polynomial model are widely used

in communication system. The Rapp model of SSPA [12] can be given as

$$G[|x_n|] = |x_n|\Big[1 + \big(\frac{|x_n|}{G_0}\big)^{2P}\Big]^{\frac{-1}{2p}} \tag{2.6}$$

where G_0 is the maximum amplifier output and p determines the smoothness of the transition from the linear region to the saturation region. The AM/PM distortion is very limited for applications.

The output of the SSPA polynomial model [13] can be expressed as

$$y_n = \sum_{k=1}^{K} \alpha_k x_n |x_n|^{k-1} \tag{2.7}$$

where K is the order of nonlinearity and α_k is the polynomial coefficients. In the polynomial model, it is sufficient to use third-order and odd-order nonlinearity for the purpose of estimation of the distortion-to-signal power ratio. Thus, the output of polynomial model can be approximated as

$$y_n \approx \alpha_1 x_n + \alpha_3 |x_n|^2 x_n \tag{2.8}$$

where the coefficients α_1 and α_3 can be obtained by (2.4) and (2.8).

2.3. Peak-to-Average Power Ratio

There are several methods to define the ratio of the peak power to the mean power such as peak envelop power (PEP), peak to mean envelope power ratio (PMEPR), PAPR, and crest factor (CF) [14]. The PEP is defined as

$$PEP = \max_t |x_t|^2 \tag{2.9}$$

where the maximum value of the peak power of complex baseband OFDM signal is used. The PMEPR is expressed as

$$PMEPR(x_t) = \frac{\max |x_t|^2}{P_{av}[x_t]} \tag{2.10}$$

where $P_{av}[\cdot]$ is the average power of the OFDM signal.

The PAPR is defined as the ratio of the peak power to the average power of the passband OFDM signal, that is,

$$PAPR(\dot{x}_t) = \frac{\max \left|\mathrm{Re}\{x_t e^{j2\pi f_c t}\}\right|^2}{P_{av}\{\mathrm{Re}[x_t e^{j2\pi f_c t}]\}} = \frac{\max |\dot{x}_t|^2}{P_{av}[\dot{x}_t]}. \tag{2.11}$$

Assume that input OFDM symbols are identically and independently distributed. Then the average power $P_{av}[\dot{x}_t]$ is σ^2.

In this dissertation, an approximation will be made in that LN samples of x_t are considered, where L is oversampling factor. The PAPR of discrete baseband OFDM signal x_n is defined as

$$PAPR(x_n) = \frac{\max_{n=0}^{LN-1} |x_n|^2}{P_{av}[x_n]}. \tag{2.12}$$

The another useful method to measure envelope variation of the OFDM signals is the crest factor, which is equivalent to the square root of PAPR as

$$CF = \sqrt{PAPR}. \tag{2.13}$$

For large N, the OFDM signal x_n can be modeled as a zero-mean complex Gaussian random variable and thus the magnitude of x_n follows Rayleigh distribution. In order to analyze PAPR, it is convenient to check

the CCDF of PAPR, i.e., the probability that the PAPR of OFDM signals exceeds a given threshold δ given as

$$P(PAPR > \delta) = 1 - (1 - e^{-\delta^2})^{\alpha N} \tag{2.14}$$

where α is usually determined as 2.8 from numerical analysis [15].

In [16], analytical CCDF expression of PAPR in OFDM systems is given by extreme value theory as

$$P(PAPR > \delta) \cong 1 - exp\left\{ -2e^{-\delta} \sqrt{\frac{\pi\delta}{NP_{av}[x_t]} \sum_{k=-K}^{K} k^2 \eta_k} \right\} \tag{2.15}$$

where η_k is the power allocated to the k-th subcarrier.

Equivalently, by simply changing δ as $\sqrt{\delta}$, the CCDF of CF is also given as

$$P(CF > \sqrt{\delta}) = 1 - (1 - e^{-\delta})^{\alpha N} \tag{2.16}$$

where α is determined as 0.64 [17].

Fig. 2.2 shows the simulation results for the CCDF of PAPR distribution for OFDM signal with $L = 4$ and $N = 256$ for various constellation, that is, QPSK, 16-QAM, and 64-QAM, which tells us that PAPR distribution is the same regardless of signal constellation.

The continuous baseband OFDM signals can be obtained by low-pass filtering the discrete baseband OFDM signals, which gives us different PAPR. In order to approximate the PAPR of the continuous baseband OFDM signals, numerical analysis for PAPR is performed with oversampling factor L. Fig. 2.3 shows the PAPR for the various oversampling

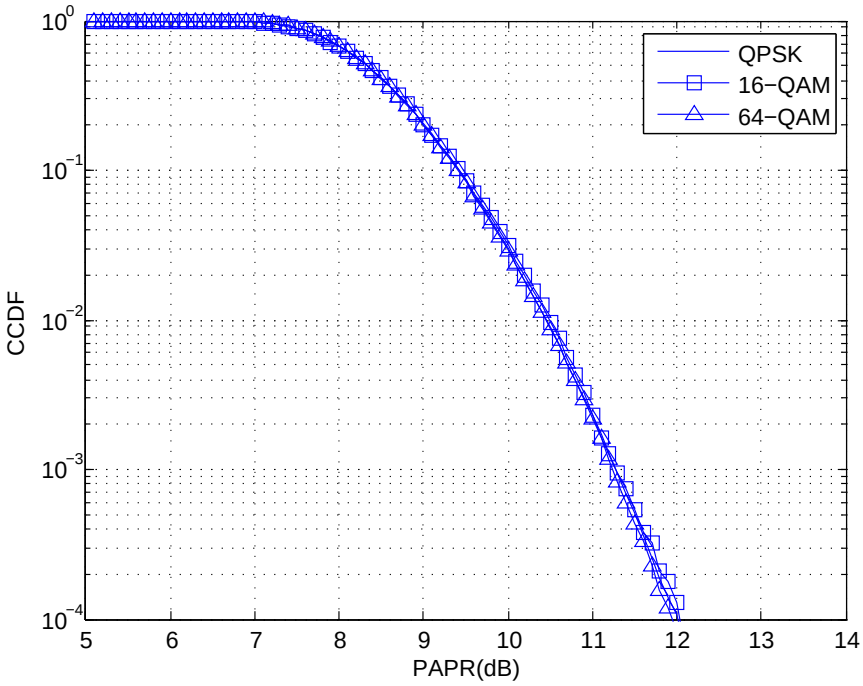

Figure 2.2: CCDF of PAPR distribution of OFDM signals with $L = 4$, $N = 256$, and various constellations QPSK, 16-QAM, and 64-QAM.

factors $L = 1, 4, 8, 12$ with $N = 256$ and 16-QAM. It is shown that the oversampling factor $L = 4$ is sufficient to approximate the PAPR of the continuous OFDM signal.

Fig. 2.4 shows the CCDF of PAPR for the various $N = 64, 128, 256, 1024$, $L = 4$, and 16-QAM. It is shown that the PAPR decreases as N decreases. Therefore, $L = 4$ and 16-QAM constellation are used in this dissertation with various number of subcarriers.

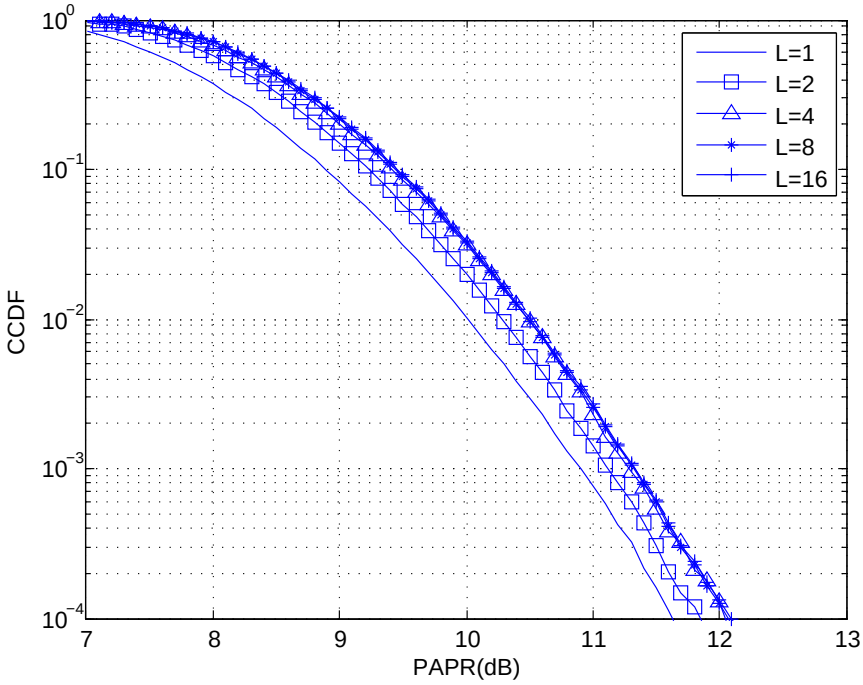

Figure 2.3: CCDF of PAPR distribution of OFDM signals with 16-QAM, $N = 256$, and various $L = 1, 2, 4, 8, 16$.

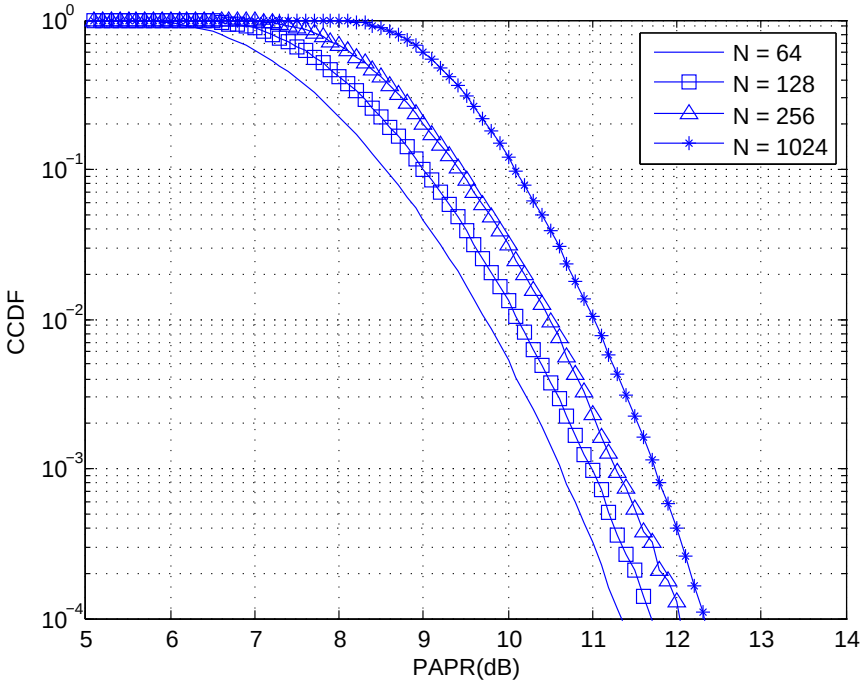

Figure 2.4: CCDF of PAPR distribution of OFDM signals with $L = 4$, 16-QAM, and various $N = 64, 128, 256, 1024$.

Chapter 3. Conventional PAPR Reduction Schemes

3.1. Clipping

The simplest PAPR reduction scheme in OFDM system is to clip the IFFTed signal with relevant threshold. The clipped signal is usually defined as

$$\bar{x}_n = \begin{cases} Ae^{j\theta_n}, & |x_n| > A \\ x_n, & |x_n| \leq A \end{cases} \tag{3.1}$$

where A is the threshold and θ_n is the phase of x_n. However, clipping the IFFTed signal causes in-band distortion and out-of-band radiation, which deteriorate BER.

In order to reduce the out-of-band radiation, clipping and filtering (CAF) scheme was introduced in [18]. The CAF scheme is the iterative scheme, that is, clipped signal is transformed to the frequency domain symbol by fast Fourier transform (FFT) to remove out-of-band radiation and it is transformed to time-domain signals by iterative IFFT again.

However, this process generates the peak regrowth and increases complexity due to IFFT and FFT operations. In [19], deep clipping scheme has been proposed, which deeply clips the high peaks to a level smaller

than a clipping level. Nevertheless, the BER is increased, because clipping cuts signals intentionally.

3.2. Selected Mapping

SLM scheme generates alternative OFDM signal vectors and selects the one with the minimum PAPR for transmission. In SLM scheme, the input symbol vector $\mathbf{X}$ is multiplied with U phase vectors given as

$$\mathbf{P}^{(u)} = [P_0^{(u)}, P_1^{(u)}, \cdots, P_{N-1}^{(u)}] \tag{3.2}$$

where $P_n^{(u)} = e^{j\phi_n^{(u)}}$ with $\phi_n \in [0, 2\pi)$ for $n = 0, \cdots, N-1$. In general, binary or quaternary elements are used for $P_k^{(u)}$, that is, $\{\pm 1\}$ or $\{\pm 1, \pm j\}$.

Using componentwise multiplication of the input symbol vector and U phase vectors, we can obtain U alternative input symbol vectors as

$$\mathbf{X}^{(u)} = \mathbf{X} \otimes \mathbf{P}^{(u)} \qquad 0 \le u \le U-1. \tag{3.3}$$

After IFFT is performed, the PAPR is calculated.

Then, an OFDM signal vector with the minimum PAPR among U alternative OFDM signal vectors is selected and transmitted. The side information for denoting the selected phase vector should be transmitted accompanying with the transmitted alternative OFDM signal vector. Modified SLM schemes have been proposed to reduce the computational complexity [20]-[22].

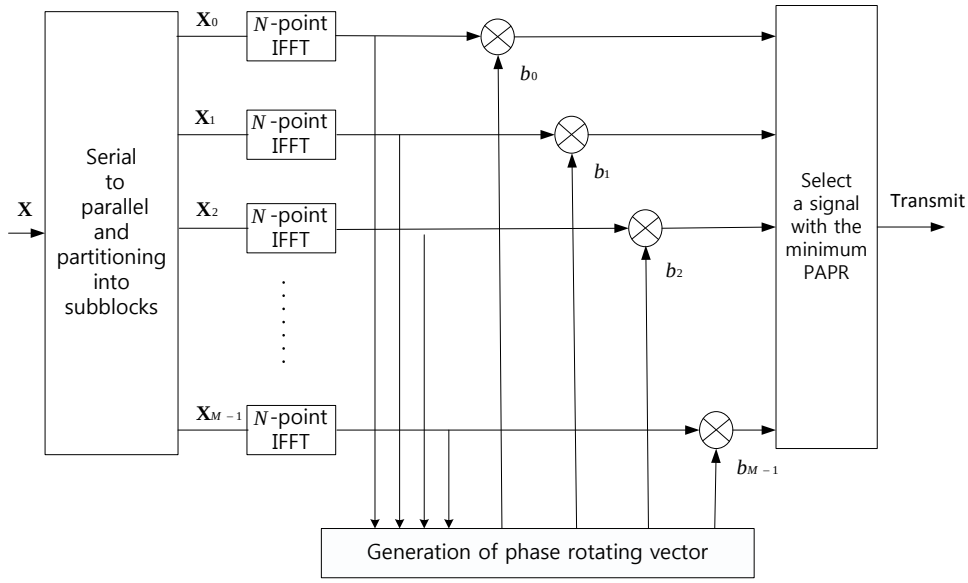

Figure 3.1: Block diagram of the conventional PTS.

3.3. Partial Transmit Sequence

In the conventional PTS scheme, an input symbol vector $\mathbf{X}$ is partitioned into M disjoint input symbol subvectors $\mathbf{X}_m = [X_{m,0}, X_{m,1}, \cdots, X_{m,N-1}]^T$, $0 \leq m \leq M-1$, that is,

$$\mathbf{X} = \sum_{m=0}^{M-1} \mathbf{X}_m \tag{3.4}$$

where $X_{m,n}$ is the m-th element of $\mathbf{X}$ or zero. There are three partitioning methods, which are random, interleaving, and adjacent partitionings [23].

By applying IFFT to each $\mathbf{X}_m$, the OFDM signal subvector $\mathbf{x}_m = [x_{m,0}, x_{m,1}, \cdots, x_{m,N-1}]^T$ is generated and each $\mathbf{x}_m$ is independently rotated by the phase rotating factor $b_m = e^{j\phi_m}$, where $\phi_m \in [0, 2\pi)$ for $m = 0, \cdots, M-1$. In practice, the phase rotating factor b_m is an element of the finite set given as

Table 3.1: An example of the OFDM signal vector at each subblock $\mathbf{x}_m$ in the PTS for $M = 4$ and $N = 8$.

$x_{m,n}$	$x_{m,0}$	$x_{m,1}$	$x_{m,2}$	$x_{m,3}$	$x_{m,4}$	$x_{m,5}$	$x_{m,6}$	$x_{m,7}$
$\mathbf{x}_0$	0	$0.04 - j0.09$	$0.13 - j0.13$	$0.21 - j0.09$	0.25	$0.21 + j0.09$	$0.13 + j0.13$	$0.04 + j0.09$
$\mathbf{x}_1$	0	$0.09 + j0.04$	$-0.13 + j0.13$	$-0.09 - j0.21$	0.25	$-0.09 + j0.21$	$-0.13 - j0.13$	$0.09 - j0.04$
$\mathbf{x}_2$	0	$0.04 - j0.09$	$-0.13 + j0.13$	$0.21 - j0.09$	-0.25	$0.21 + j0.09$	$-0.13 - j0.13$	$0.04 + j0.09$
$\mathbf{x}_3$	0.25	$-0.09 + j0.21$	$0.13 + j0.13$	$0.09 - j0.04$	0.25	$0.09 + j0.04$	$0.13 - j0.13$	$-0.09 - j0.21$
$\lvert\mathbf{x}_n\rvert$	-0.25	$-0.09 + j0.21$	$0.13 + j0.13$	$0.09 - j0.04$	0.25	$0.09 + j0.04$	$0.13 - j0.13$	$-0.09 - j0.21$

$$b_m \in \{e^{j2\pi l/W} \mid l = 0, 1, \cdots, W-1\} \tag{3.5}$$

where W is the number of allowed phase rotating factors. Then, the phase rotating vectors are defined as $\mathbf{b}^{(u)} = [b_0^{(u)}, b_1^{(u)}, \cdots, b_{M-1}^{(u)}]$, $u = 0, 1, \cdots, U-1$, and the u-th alternative OFDM signal vector $\mathbf{x}^{(u)}$ is generated as

$$\mathbf{x}^{(u)} = [x_0^{(u)}, x_1^{(u)}, \cdots, x_{N-1}^{(u)}]^T = \sum_{m=0}^{M-1} b_m^{(u)} \mathbf{x}_m, u = 0, 1, \cdots, U-1 \tag{3.6}$$

where U is the number of alternative OFDM signal vectors.

Since the phase rotating factors $b_0^{(u)}$ for the first subblock $\mathbf{x}_0$ are fixed to 1, we have $U = W^{M-1}$. Finally, the optimal OFDM signal vector $\mathbf{x}^{(u_{opt})}$ with the minimum PAPR is selected and transmitted. Fig. 3.1 shows a block diagram of the conventional PTS scheme.

An example of the conventional PTS scheme is given for $M = 4$, $W = 2$, and $N = 8$. The input symbol vector is given as $\mathbf{X} = [1, -1, 1, -1, -1, 1, -1, -1]$, which is divided into four subblocks with the adjacent method, that is,

$\mathbf{X}_0 = [1, -1, 0, 0, 0, 0, 0, 0]$, $\mathbf{X}_1 = [0, 0, 1, -1, 0, 0, 0, 0]$, $\mathbf{X}_2 = [0, 0, 0, 0, -1, 1, 0, 0]$, $\mathbf{X}_3 = [0, 0, 0, 0, 0, 0, -1, -1]$.

After being transformed by IFFT, the OFDM signal vector subblock $\mathbf{x}_m$ is shown in Table 3.1. Since the phase rotating factor b_m is selected in $\{\pm 1\}$, we have $U = W^{M-1} = 8$ phase rotating vectors as $\mathbf{b}^{(0)} = [1, 1, 1, 1]$, $\mathbf{b}^{(1)} = [1, -1, 1, 1]$, $\mathbf{b}^{(2)} = [1, 1, -1, 1]$, $\mathbf{b}^{(3)} = [1, 1, 1, -1]$, $\mathbf{b}^{(4)} = [1, -1, -1, 1]$, $\mathbf{b}^{(5)} = [1, -1, 1, -1]$, $\mathbf{b}^{(6)} = [1, 1, -1, -1]$, and $\mathbf{b}^{(7)} = [1, -1, -1, -1]$. Using (3.6), we can generate $U = 8$ alternative OFDM signal vectors by rotating $\mathbf{x}_m$ with phase rotating vectors, that is, $\mathbf{x}^{(u)} = b_0^{(u)}\mathbf{x}_0 + b_1^{(u)}\mathbf{x}_1 + b_2^{(u)}\mathbf{x}_2 + b_3^{(u)}\mathbf{x}_3$, $u = 0, 1, \cdots, 7$.

Two disadvantages of the conventional PTS scheme are loss of data transmission rate due to the side information and large computational complexity. The side information of $\lceil \log_2 W^{M-1} \rceil$ bits for the selected phase rotating vector should be transmitted accompanying with the selected alternative OFDM signal vector. It was proposed to transmit OFDM signal vectors of PTS scheme without side information [24]-[26].

The computational complexity of PTS increases exponentially with the number of the subblocks, which comes from many IFFTs and lots of alternative OFDM signal vectors. The computational complexity of PTS scheme is determined by the following three parts;

a) M IFFTs for M subblocks.

b) Generation of U alternative OFDM signal vectors.

c) Computation and comparison of PAPRs of U alternative OFDM signal

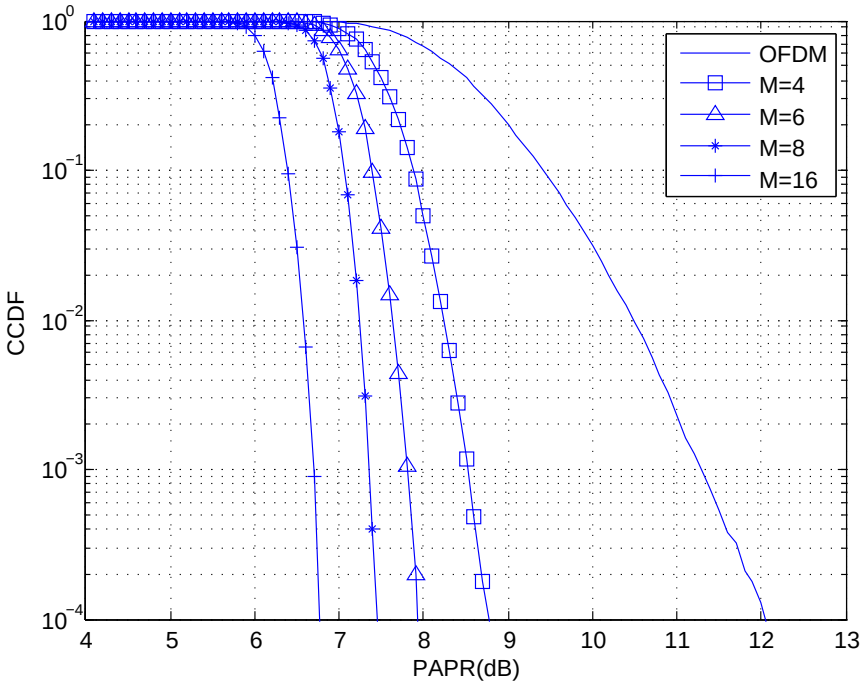

Figure 3.2: Comparison of PAPR reduction performance of PTS scheme with 16-QAM, $L = 4$, $W = 4$, $N = 256$, and various $M = 4, 6, 8, 16$.

vectors.

Fig. 3.2 shows the comparison of PAPR reduction performance of PTS scheme with 16-QAM, $L = 4$, $W = 4$, $N = 256$, and various $M = 4, 6, 8, 16$. As the number of subblocks M is larger, the PAPR reduction performance is getting better. Note that as M increases, the computational complexity of IFFT and multiplications and additions for the alternative OFDM signal vectors also increases.

Fig. 3.3 shows the comparison of PAPR reduction performance of PTS scheme with 16-QAM, $M = 4$, $N = 256$, $L = 4$, and various $W = 2, 4, 6, 8$.

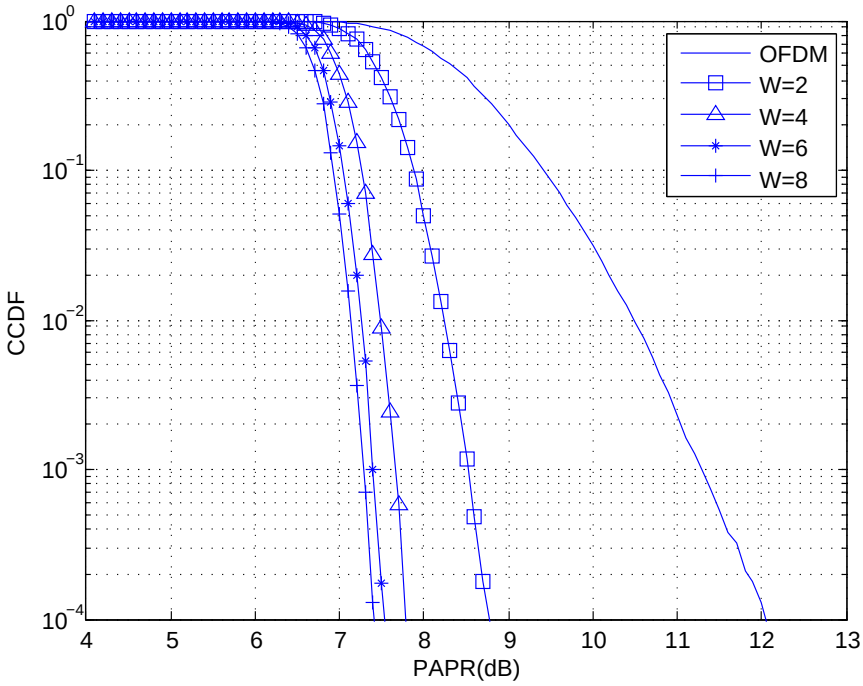

Figure 3.3: Comparison of PAPR reduction performance of PTS scheme with 16-QAM, $M = 4$, $N = 256$, $L = 4$, and various $W = 2, 4, 6, 8$.

It is shown that the PAPR reduction performance is getting better as W is larger, but the number of bits for side information also increases.

Fig. 3.4 shows the comparison of PAPR performance of OFDM with $M = 4$, $L = 4$, $N = 256$, $W = 4$, and random, interleaving, and adjacent partitionings. The random partitioning shows the best PAPR reduction performance than any other partitioning methods. Thus, the random partitioning method is only used in this dissertation.

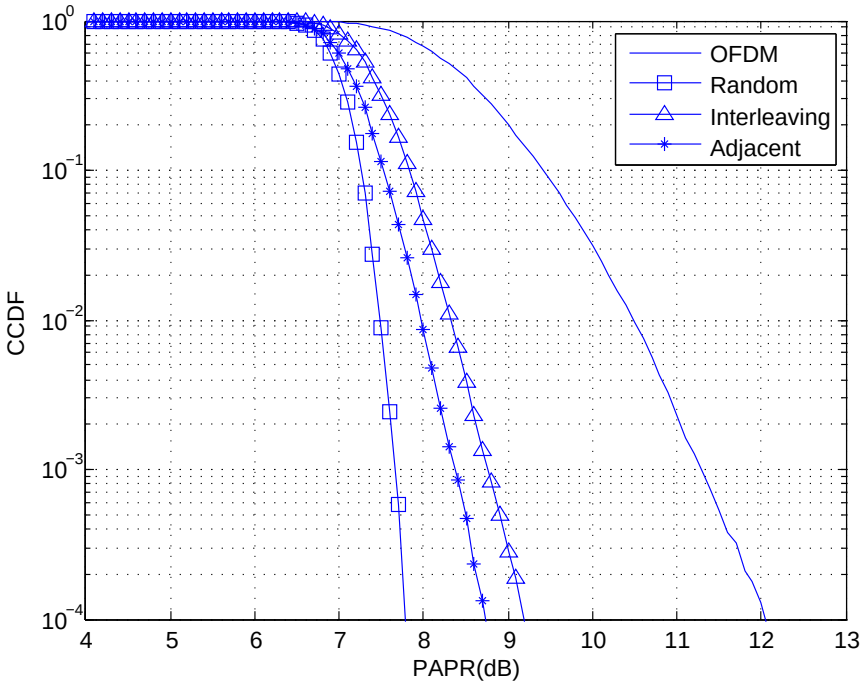

Figure 3.4: Comparison of PAPR performance of OFDM with $M = 4$, $L = 4$, $N = 256$, $W = 4$ and random, interleaving, and adjacent partitionings.

3.4. Low-Complexity PTS Schemes

The PTS scheme requires the exhaustive search to find the best phase rotating vectors to minimize the PAPR of the OFDM signal vector. In order to reduce the computational complexity, three types of low-complexity PTS schemes have been considered. The first type of PTS scheme is to reduce the computational complexity for IFFTs which uses the modified IFFTs [27]. The next low-complexity PTS schemes reduce the number of U alternative OFDM signal vectors such as iterative PTS (IPTS) [28], sphere decoding (SD-PTS) [29], suboptimal PTS [30], and PTS using sequences

[31][32]. Considering the PAPR problem of the PTS scheme as combinatorial optimization (CO) problem, heuristic algorithms have been proposed to reduce the number of phase rotating vectors for the PTS scheme, which includes the simulated anealing (SA) [33], the particle swarm optimization (PSO-PTS) [34], the genetic algorithm [35], the tabu search algorithm [36], and the artificial bee colony algorithm (ABC-PTS) [37]. And the last type of low-complexity PTS is to reduce the number of time-domain samples used for peak power computation in each alternative OFDM signal vectors [38]-[40].

3.4.1. Reduction of the Number of Alternative OFDM Signal Vectors Using Sphere Decoding

Low-complexity PTS scheme using sphere decoding (SD-PTS) is proposed in [29]. The power of $x_n^{(u)}$ is written as

$$\left|x_n^{(u)}\right|^2 = \mathbf{b}^H \mathbf{F}_n^H \mathbf{F}_n \mathbf{b} - \alpha^2 M \tag{3.7}$$

where α is an arbitrary nonzero real number, $(\cdot)^H$ denotes the conjugate transpose, and $\mathbf{F}_n$ is an upper-triangular matrix given as

$$\mathbf{F}_n = \begin{pmatrix} F_{1,1}^n & \cdots & F_{1,M}^n \\ 0 & F_{2,2}^n & F_{2,M}^n \\ \vdots & \ddots & \vdots \\ 0 & 0 & F_{M,M}^n \end{pmatrix}.$$

In order to find the PAPR of the OFDM signal, the power of $x_n^{(u)}$ is subject to the following constraint:

$$||\mathbf{F}_n\mathbf{b}||^2 < \mu^2 + \alpha^2 M \tag{3.8}$$

where μ is the some positive number.

Only those phase rotating vectors that lie inside the sphere of radius $\mu^2 + \alpha^2 M$ are searched in SD-PTS, which can reduce the computational complexity of the search by limiting the sphere radius.

3.4.2. Reduction of the Number of Alternative OFDM Signal Vectors Using ABC Algorithm

When the number M of subblocks is fixed, the generation of U alternative OFDM signal vectors is mainly considered for reducing the computational complexity of the PTS scheme. The search problem of PTS as a CO problem enables us to adapt efficient search algorithms.

We can formulate the vector search of PTS as a binary CO problem, that is;

Minimize

$$f(\mathbf{b}) = \frac{\max_{n=0}^{N-1} \left| \sum_{m=0}^{M-1} b_m x_{m,n} \right|^2}{E[|x_n|^2]} \tag{3.9}$$

subject to

$$\mathbf{b} \in \{\pm 1\}^{M-1}. \tag{3.10}$$

In order to solve the optimization problem, the modified ABC algorithm PTS (ABC-PTS) for PAPR reduction is proposed in [37]. In the ABC

algorithm, the bees search the food source position which represents a possible solution to the problem to be optimized. And the nectar amount of a food source corresponds to the quality of the associated solution.

At first, ABC algorithm is to set food source positions randomly, which is the same as the phase rotating vectors of PTS scheme. A food source position from the previous one is produced by

$$b_{nl}^{(u)} = b_{nl} + \beta_{nl}(b_{nl} - b_{kl}) \tag{3.11}$$

where $l \in \{1, 2, \ldots, M\}$ and $k \in \{1, 2, \ldots, J\}$, $i \neq k$, J is the number of food sources, and β is a random number between $[-1, 1]$.

Next, corresponding nectar amount in the food source is calculated. The nectar amount is considered as the PAPR of alternative OFDM signal vectors. If the nectar amount of a food source is much lower than other food sources, it is abandoned and replaces another food source. This steps are repeated until the value of limit meets.

The procedure of the RC-PTS schemes is summarized as follows.

1) Initialize food source positions which are the same as the initial phase rotating vectors in PTS.

2) Calculate the nectar amount which is the PAPR of alternative OFDM signal vectors in PTS scheme.

3) Find the abandoned food source and replace it to a neighbour food source position.

4) Iterate this steps until pre-determined limit meets.

5) Memorize the position of the best food source.

3.4.3. PTS Scheme with Dominant Time-Domain Samples

Reduced-complexity PTS (RC-PTS) scheme has been proposed to reduce the computational complexity of the conventional PTS scheme [38]. In the RC-PTS, the summed power of the n-th time-domain samples in each subblock is considered to find the indices of the dominant time-domain samples with power larger than preset threshold of the alternative OFDM signal vectors.

This approach is useful in that it does not reduce the number of alternative OFDM signal vectors but reduce the time-domain samples of the alternative OFDM signal vectors to find the peak value.

The power of $x_n^{(u)}$ is written as

$$|x_n^{(u)}|^2 = \left| \sum_{m=0}^{M-1} b_m^{(u)} x_{m,n} \right|^2 = \underbrace{\sum_{m=0}^{M-1} |x_{m,n}|^2}_{Q_n} + \underbrace{\sum_{m_1=0}^{M-1} \sum_{\substack{m_2=0 \\ m_2 \neq m_1}}^{M-1} (b_{m_1}^{(u)} x_{m_1,n})(b_{m_2}^{(u)} x_{m_2,n})^*}_{B_n^{(u)}} \tag{3.12}$$

where Q_n is a metric which is independent of the phase rotating vector for a given $\mathbf{X}$ and $B_n^{(u)}$ is the cross term of the $|x_n^{(u)}|^{(2)}$ affected by the phase rotating vector. Let $\mathbf{S}_Q$ be the set of indices defined as

$$\mathbf{S}_Q = \{n \mid Q_n \geq \gamma, \quad 0 \leq n \leq N-1\} \tag{3.13}$$

where γ is the threshold of Q_n. Then, only the samples $x_n^{(u)}$ with $n \in \mathbf{S}_Q$ are multiplied with phase rotating vectors to compute the PAPR of alternative OFDM signal vectors.

Thus, the RC-PTS can reduce the computational complexity by only considering a subset of the time-domain samples of OFDM signal vectors in order to find an OFDM signal vector with the minimum PAPR. The optimal OFDM signal vector $\mathbf{x}^{(u_{opt})}$ is obtained as

$$u_{opt} = \arg \min_{u=0}^{U-1} \frac{\max_{n \in \mathbf{S}_Q} \left| \sum_{m=0}^{M-1} b_m^{(u)} x_{m,n} \right|^2}{E[|x_n|^2]}. \tag{3.14}$$

The procedure of the RC-PTS schemes is summarized as follows.

1) Evenly partition the input symbol block $\mathbf{X}$ into M disjoint subblocks.

2) Find $\mathbf{x}_m = [x_{m,0}\ x_{m,1}\ \cdots\ x_{m,N-1}]^T$ by IFFT.

3) Compute $\mathbf{Q} = \{Q_0, Q_1, \cdots, Q_{N-1}\}$, where $Q_n = \sum_{m=0}^{M-1} |x_{m,n}|^2$.

4) Record the time indices n such that $Q_n > \gamma$ as a set $\mathbf{S}_Q$.

5) Only the samples $x_n^{(u)}$ with $n \in \mathbf{S}_Q$ are used to compute the PAPR.

6) Select the optimal vector $\mathbf{b}^{(u_{opt})}$.

7) Generate $\mathbf{x}^{(u_{opt})}$ using the phase rotating vector $\mathbf{b}^{(u_{opt})}$ and transmit it.

In [38], the PAPR reduction performance of RC-PTS with small dominant time-domain samples is shown to be the same as that of the conventional PTS.

Chapter 4. A New Low-Complexity PTS Schemes Based on Successive Local Search Using Sequences

4.1. Introduction

A new PTS scheme with low computational complexity is proposed, where two search steps are taken to find a subset of phase rotating vectors showing good PAPR reduction performance. In the first step, sequences with low correlation are used as phase rotating vectors for PTS scheme, which are called the initial phase vectors. In the second step, local search is performed based on the initial phase vectors to find additional phase rotating vectors which show good PAPR reduction performance. Numerical analysis shows that the proposed PTS scheme achieves better PAPR reduction performance with significantly reduced computational complexity than the existing low-complexity PTS schemes.

This chapter is organized as follows. In Section 4.2, a new PTS scheme with two sequential steps using sequences with low correlation property is proposed to reduce computational complexity of the PTS scheme. In Section 4.3, computational complexity of the proposed PTS scheme is compared and then, numerical analysis is shown. Finally, conclusion is given in Section 4.4.

4.2. A New PTS Scheme Based on Sequences with Good Correlation

In this section, a new PTS scheme with two search steps is proposed, where the initial phase vectors are generated by using sequences with good correlation property in the first step and then additional phase rotating vectors are generated by changing one symbol of the initial phase vectors in the second step.

4.2.1. First Step: Initial Phase Vectors

Kasami sequences [41] and quaternary sequences of Family A [42] are considered as initial phase vectors for the proposed PTS scheme. Kasami sequences are important binary sequences having very low cross-correlation values, which are generated by taking the modulo-2 sum of a binary m-sequence and its decimated sequences [41]. There are two different sets of Kasami sequences, a large set and a small set. In this chapter, we use a small set of Kasami sequences having an optimal correlation property with respect to Welch bound.

To generate a small set of Kasami sequences, we begin with a binary m-sequence μ of period $2^r - 1$ for even r and a shorter-period sequence $\mu^{'}$ obtained by decimating μ by $2^{r/2} + 1$. Note that the resulting shorter-period sequence $\mu^{'}$ is an m-sequence of period $2^{r/2} - 1$. Then a small set of Kasami sequences is generated by taking the modulo-2 sum of μ and all the cyclically shifted sequences of $\mu^{'}$, which results in $2^{r/2}$ binary sequences of period $2^r - 1$. The total number of Kasami sequences and

their all cyclically shifted sequences is $2^{r/2}(2^r-1)$. Thus, the total number N_K of phase rotating vectors selected from them should satisfy

$$N_K \leq 2^{r/2}(2^r-1). \tag{4.1}$$

These N_K binary sequences are used as initial phase vectors for the proposed PTS scheme, where the alphabet size for the phase rotating factors is $W = 2$.

A family of quaternary sequences over Z_4 with optimal correlation property, called Family A, has been proposed in [42], which consists of $2^r + 1$ quaternary sequences of period $2^r - 1$. Clearly, the total number of quaternary sequences of Family A and their all cyclically shifted sequences is $(2^r + 1)(2^r - 1)$. Then, the total number N_Q of initial phase vectors selected from them should satisfy

$$N_Q \leq (2^r + 1)(2^r - 1). \tag{4.2}$$

For example, the Kasami and quaternary sequences of period 15 can be used as the initial phase vectors for the proposed PTS scheme with $M = 16$, where the phase rotating factor $b_0^{(u)}$ for the first subblock is fixed to one. In this case, the maximum number of binary initial phase vectors of length 15 is $N_K = 60$ from (4.1) and the maximum number of quaternary initial phase vectors of length 15 is $N_Q = 225$ from (4.2). However, it is not guaranteed to find a good solution for the proposed PTS scheme only by using these initial phase vectors. Therefore, in the second step, one symbol of each initial phase vector is further changed to

generate additional phase rotating vectors. Note that, by using sequences with low correlation as initial phase vectors, the search in the second step becomes more efficient.

4.2.2. Second Step: Local Search

Suppose that P_0 initial phase vectors are generated in the first step, where $P_0 = N_K$ or N_Q. Then P_1 vectors giving the smallest PAPRs are selected from these P_0 initial phase vectors, $0 < P_1 \leq P_0$, which are used to generate additional phase rotating vectors by changing one symbol from each of them, called *local search*.

This local search will be explained by using an example. Assume that the phase rotating factor for the second subblock of the alternative OFDM signal vector $\mathbf{x}^{(u)}$ is changed from $b_1^{(u)}$ to $b_1^{(u')}$, where $b_1^{(u')}$ can take any phase rotating factor except $b_1^{(u)}$. Then the additional alternative OFDM signal vector $\mathbf{x}^{(u')}$ can easily be obtained as

$$\mathbf{x}^{(u')} = \mathbf{x}^{(u)} + (b_1^{(u')} - b_1^{(u)})\mathbf{x}_1 \tag{4.3}$$

without summing all $\mathbf{x}_m$'s weighted by a new phase rotating vector $\mathbf{b}^{(u')}$. Compared with the conventional PTS, the computational complexity to obtain additional alternative OFDM signal vectors in (4.3) can be substantially reduced. The phase rotating factor for the second subblock of other alternative OFDM signal vector can be changed in the same fashion to generate additional alternative OFDM signal vectors. Then, $P_1(W-1)$ additional phase rotating vectors are generated by changing the phase ro-

Table 4.1: P_m values for 900 phase rotating vectors in the proposed PTS scheme using Kasami sequences when $M = 16$.

P_0	$P_1(W-1)$	$P_2(W-1)$	$P_3(W-1)$
60	60×1	60×1	60×1
$P_4(W-1)$	$P_5(W-1)$	$P_6(W-1)$	$P_7(W-1)$
60×1	60×1	60×1	60×1
$P_8(W-1)$	$P_9(W-1)$	$P_{10}(W-1)$	$P_{11}(W-1)$
60×1	60×1	60×1	60×1
$P_{12}(W-1)$	$P_{13}(W-1)$	$P_{14}(W-1)$	$P_{15}(W-1)$
60×1	60×1	30×1	30×1

tating factor for the second subblock. After calculating PAPRs of these $P_1(W-1)$ alternative OFDM signal vectors and comparing PAPRs of total $P_1 W$ alternative OFDM signal vectors, we can select P_2 phase rotating vectors giving the smallest PAPRs.

Similar to the second block case, $P_2(W-1)$ additional phase rotating vectors are generated from these P_2 phase rotating vectors by changing the phase rotating factor for the third subblock, and the same comparison and selection are performed. This procedure continues up to the last subblock and the total number T of phase rotating vectors in the proposed PTS scheme becomes

$$T = P_0 + (W-1) \sum_{m=1}^{M-1} P_m. \tag{4.4}$$

Extensive simulation is performed to find P_m for good PAPR reduction performance. As an example, for the case of $M = 16$, the number $P_m(W-1)$ of additional phase rotating vectors generated by local search for each subblock is listed in Table 4.1, where a small set of Kasami sequences of length 15 and local search are used to select $T = 900$ phase rotating vectors out of $2^{15} = 32768$ binary vectors.

4.3. Computational Complexity and Simulation Results

4.3.1. Comparison of Computational Complexity

The computational complexity of PTS scheme is determined by the following three parts:

a) M IFFTs for M subblocks.

b) Generation of U alternative OFDM signal vectors.

c) Computation and comparison of PAPRs of U alternative OFDM signal vectors.

In general, when M subblocks is fixed, the computational complexity for the part a) is also fixed, and the part b) is mainly considered for reducing the computational complexity of the PTS scheme, while the computational complexity of part c) is negligible.

In order to reduce the computational complexity, the optimal search has been proposed in [29], where the computational complexity is reduced by restricting searching among the alternative OFDM signal vectors inside a sphere by using sphere decoding algorithm. Recently, combinatorial optimization algorithms including ABC-PTS [37] and parallel TS-PTS [36] have been used to efficiently search a good subset of phase rotating vectors for the PTS scheme to further reduce the computational complexity of the part b).

Table 4.2 compares the computational complexity of the conventional PTS, the optimal search, the parallel TS-PTS, ABC-PTS, and the proposed PTS scheme for $M = 16$, $L = 4$, $W = 2$, $N = 256$, and $T = 900$. Since the computational complexity due to the complex additions shows the same tendency, only the complex multiplications for generating alternative OFDM signal vectors in the part b) are considered in Table 4.2.

The optimal search algorithm in [29] searches the alternative OFDM signal vectors inside a sphere corresponding to $\gamma^2 = 6.8$, which results in generating $A = 16253$ alternative OFDM signal vectors on average. Note that while the conventional PTS and the optimal search generate $W^{M-1} = 2^{15} = 32768$ and $A = 16253$ alternative OFDM signal sequences, respectively, the other low-complexity PTS schemes generate $T = 900$ alternative OFDM signal vectors. Table 4.2 shows that, compared with the number of complex multiplications required by the conventional PTS, the optimal search requires 49.6% of computational complexity and each of parallel TS-PTS and ABC-PTS requires 2.75% of computational complexity, whereas the proposed PTS scheme requires only 0.42% of computational complexity by using P_m in Table 4.1. Clearly, the proposed PTS scheme shows the lowest computational complexity among other low-complexity PTS schemes.

In the next subsection, it will be shown that the proposed PTS scheme can give almost the same PAPR reduction performance as the conventional PTS scheme.

Table 4.2: Comparison of computational complexity of the proposed PTS scheme and other PTS schemes for $M = 16$, $L = 4$, $W = 2$, $N = 256$, $A = 16253$ and $T = 900$.

PTS schemes	No. of complex multiplications	Percentage
Conventional PTS	$(M-1)LNW^{M-1}$	100%
Optimal search	$(M-1)LNA$	49.6%
Parallel TS-PTS	$(M-1)LNT$	2.75%
ABC-PTS	$(M-1)LNT$	2.75%
Proposed PTS	$(M-1)LNP_0$ $+LN(W-1)\sum_{m=1}^{M-1} P_m$	0.42%

4.3.2. Simulation Results

Fig. 4.1 compares the PAPR reduction performance of the conventional PTS scheme, the proposed PTS scheme with Kasami sequences (K-PTS), and the proposed PTS scheme with quaternary sequences of Family A (Q-PTS) for $M = 16$, $L = 4$, $N = 256$, and 16-QAM. Fig. 4.1 shows that Q-PTS outperforms K-PTS. Note that Q-PTS with $T = 1200$ shows almost the same PAPR reduction performance as the conventional PTS with $W = 2$ and $U = 32768$.

Fig. 4.2 compares the PAPR reduction performance of the conventional PTS, the optimal search, ABC-PTS, and the parallel TS-PTS for $W = 2$, the random search (RS) for $W = 2$ and 4, and the proposed K-PTS and Q-PTS. An OFDM system with $M = 16$, $L = 4$, $N = 256$, and 16-QAM is considered. For the optimal search, $A = 16253$ alternative OFDM signal vectors are generated and for other low-complexity PTS schemes, $T = 900$ alternative OFDM signal vectors are generated. It can be seen that the PAPRs of the random search at $CCDF = 10^{-3}$ for $W = 2$ and

$W = 4$ are the same as 7.15dB. Meanwhile, the PAPRs of ABC-PTS, the parallel TS-PTS, K-PTS, and Q-PTS are 7.02dB, 6.85dB, 6.9dB, and 6.72dB at $CCDF = 10^{-3}$, respectively. As expected, the optimal search shows identical PAPR reduction performance with the conventional PTS scheme. Compared with other PTS schemes, the proposed PTS scheme shows similar or better PAPR reduction performance with much lower computational complexity as given in Table 4.2.

4.4. Conclusion

In this chapter, a new two-step search algorithm for PTS scheme is proposed to reduce the computational complexity. In the first step, sequences with good correlation property such as Kasami and quaternary sequences are used as the initial phase vectors. In the second step, by using the initial phase vectors, local search is performed for further searching the phase rotating vectors with very low computational complexity. Numerical analysis shows that the proposed PTS scheme can achieve almost the same PAPR reduction performance as the conventional PTS scheme with much lower computational complexity than other low-complexity PTS schemes.

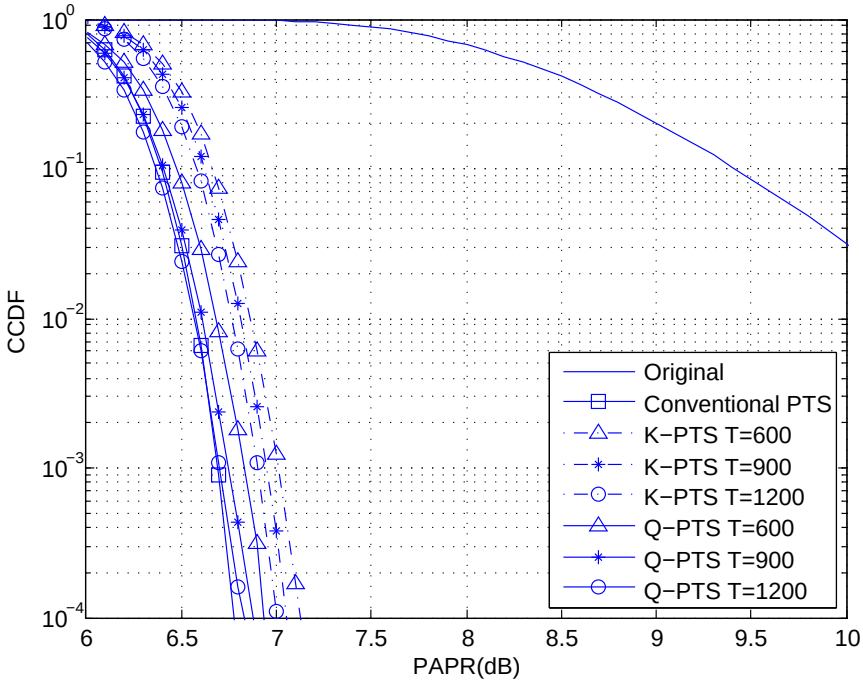

Figure 4.1: Comparison of PAPR reduction performance of the conventional and the proposed PTS schemes using various sequences with $M = 16$, $L = 4$, $N = 256$, and 16-QAM.

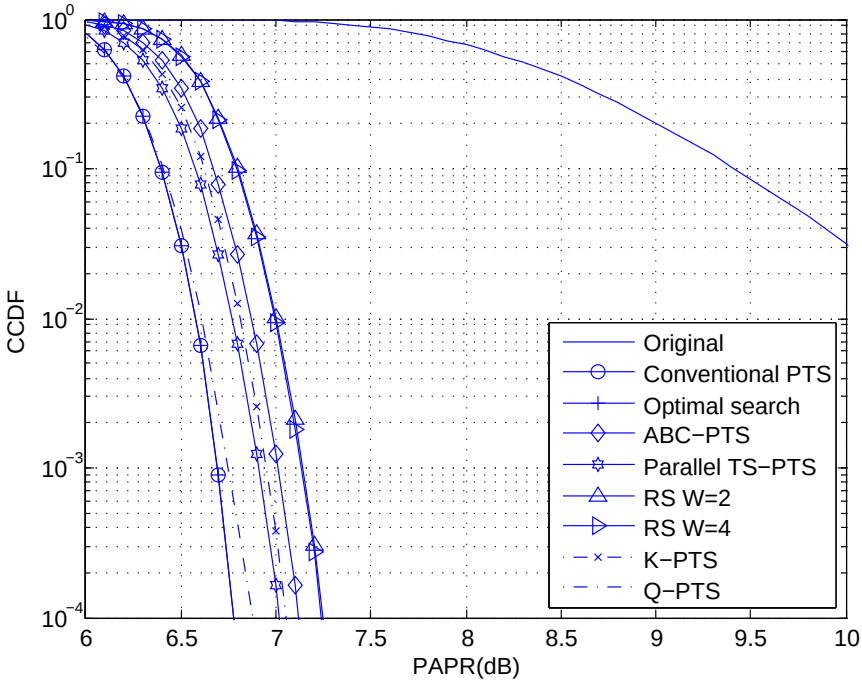

Figure 4.2: Comparison of PAPR reduction performance of various PTS schemes with $M = 16$, $L = 4$, $T = 900$, $N = 256$, and 16-QAM.

Chapter 5. Low-Complexity PTS Schemes Using Dominant Time-Domain Samples

5.1. Introduction

The PTS scheme requires an exhaustive search over all combinations of allowed phase rotating vectors, whose complexity increases exponentially with the number of subblocks. Many low-complexity PTS schemes have been proposed to simplify search of the optimal phase rotating vector over many phase rotating vectors in the PTS scheme.

The RC-PTS [38] was proposed to reduce the computational complexity, which selects dominant time-domain samples based on symbol powers and then, by using those selected samples, find alternative OFDM signal vector with the minimum PAPR. In this chapter, two new metrics are proposed to select dominant time-domain samples in the RC-PTS. For further lowering the computational complexity, dominant time-domain samples are sorted in decreasing order using their metric values and then the power of each sample is compared with the minimum PAPR of the previously examined alternative OFDM signal vectors. Simulation results confirm that the proposed PTS schemes show identical PAPR reduction performance with substantially reduced computational complexity, compared to the conventional PTS scheme.

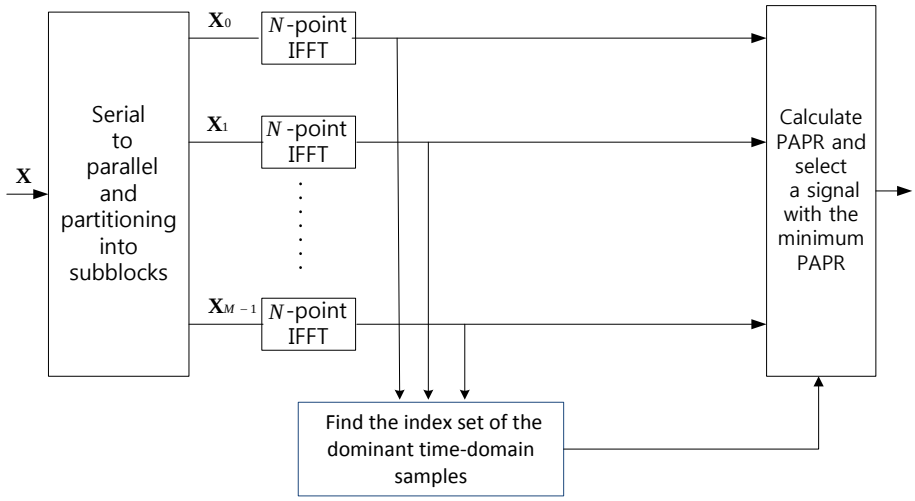

Figure 5.1: The block diagram of the PTS scheme using the dominant time-domain samples.

The rest of the chapter is organized as follows. Low-complexity PTS schemes using new metrics and sorting method are proposed in Section 5.2. In Section 5.3, the computational complexity of the proposed PTS schemes is analyzed and the simulation results are provided. Finally, conclusions are given in Section 5.4.

5.2. New Low-Complexity PTS Schemes

5.2.1. Selection of Dominant Time-Domain Samples Using New Metrics

Fig. 5.1 shows the block diagram of the PTS scheme using the dominant time-domain samples. In the RC-PTS scheme, more accurate PAPR estimation is achieved by using a lower threshold, which selects more samples, but it gives rise to an increase in the computational complexity. In

this subsection, two new metrics are proposed by analyzing the crest factor of alternative OFDM signal vectors, which show better PAPR estimation with less dominant time-domain samples compared with the RC-PTS scheme.

To select the alternative OFDM signal vector with the minimum PAPR, the magnitude of the n-th sample over all alternative OFDM signal vectors should be calculated as

$$|x_n^{(u)}| = \left| \sum_{m=0}^{M-1} b_m^{(u)} x_{m,n} \right|. \tag{5.1}$$

However, $|x_n^{(u)}|$ clearly depends on the phase rotating vector $\mathbf{b}^{(u)}$ and, in order to select dominant time-domain samples, metrics which are independent of phase rotating vector are needed similar to Q_n in (3.12) for the RC-PTS scheme. Therefore, two new metrics will be proposed by analyzing $|x_n^{(u)}|$.

The magnitude of $x_n^{(u)}$ can be rewritten as

$$|x_n^{(u)}| = \left| \sum_{m=0}^{M-1} |x_{m,n}| \, e^{(j\theta_{m,n} + j\phi_m^{(u)})} \right| \tag{5.2}$$

where $\theta_{m,n}$ and $\phi_m^{(u)}$ are the phases of $x_{m,n}$ and $b_m^{(u)}$, respectively. The first proposed metric Y_n is obtained by removing the phase part of the summand in (5.2) as

$$Y_n = \sum_{m=0}^{M-1} |x_{m,n}| \, . \tag{5.3}$$

Clearly, $Y_n \geq |x_n^{(u)}|$ and as W increases, Y_n approaches to the real maximum magnitude $\max_{u=0}^{U-1} |x_n^{(u)}|$, whereas the metric Q_n in RC-PTS does

not approach to $\max_{u=0}^{U-1}|x_n^{(u)}|$ due to the term $B_n^{(u)}$. Therefore, for large W, it is highly probable that the dominant time-domain samples obtained by using Y_n give real peak and through numerical analysis, it will be shown that the proposed low-complexity PTS scheme using Y_n outperforms the RC-PTS scheme using Q_n even for small W.

In order to propose the second metric, $|x_n^{(u)}|$ is rewritten as

$$|x_n^{(u)}| = \left| \sum_{m=0}^{M-1} b_m^{(u)} (\mathrm{Re}\{x_{m,n}\} + j\mathrm{Im}\{x_{m,n}\}) \right| \tag{5.4}$$

where $\mathrm{Re}\{x_{m,n}\}$ and $\mathrm{Im}\{x_{m,n}\}$ are the real and imaginary parts of $x_{m,n}$, respectively. Then, the second proposed metric A_n is defined as

$$A_n = \left| \sum_{m=0}^{M-1} (|\mathrm{Re}\{x_{m,n}\}| + j\,|\mathrm{Im}\{x_{m,n}\}|) \right|. \tag{5.5}$$

In case of $W = 2$, it is clear that $A_n \geq |x_n^{(u)}|$ and A_n is equal to the real maximum magnitude $\max_{u=0}^{U-1}|x_n^{(u)}|$, when the signs of real (and imaginary) parts of samples from subblocks are the same. However, if $W > 2$, $A_n \geq |x_n^{(u)}|$ is not always true.

Now, the sets of indices of the dominant time-domain samples selected by using the metrics Y_n and A_n are defined as

$$\begin{aligned} \mathbf{S}_Y &= \{n \mid Y_n \geq Th_Y\} \\ \mathbf{S}_A &= \{n \mid A_n \geq Th_A\} \end{aligned} \tag{5.6}$$

where Th_Y and Th_A are the thresholds on Y_n and A_n, respectively. The cardinality of $\mathbf{S}_Y$ and $\mathbf{S}_A$ is denoted by $|\mathbf{S}_Y| = K_Y$ and $|\mathbf{S}_A| = K_A$,

respectively. In general, the threshold is determined by considering the tradeoff between the computational complexity and the PAPR reduction performance. Note that only the dominant time-domain samples with the indices in $\mathbf{S}_Y$ or $\mathbf{S}_A$ are multiplied with the phase rotating vectors to find the alternative OFDM signal vector with the minimum PAPR. Thus, the computational complexity of the proposed PTS scheme substantially reduces.

5.2.2. Sorting of Dominant Time-Domain Samples

For further lowering the computational complexity of the low-complexity PTS schemes in Subsection 5.2.1 without degrading the PAPR reduction performance, the selected dominant time-domain samples are sorted in decreasing order using their metric values. Thus, the sorted index sets in decreasing order from $\mathbf{S}_Y$ and $\mathbf{S}_A$ are given as

$$\begin{aligned} \hat{\mathbf{S}}_Y &= \{p_0, \cdots, p_k, \cdots, p_{K_Y-1}\}, \qquad p_k \in \mathbf{S}_Y \\ \hat{\mathbf{S}}_A &= \{q_0, \cdots, q_k, \cdots, q_{K_A-1}\}, \qquad q_k \in \mathbf{S}_A. \end{aligned} \tag{5.7}$$

Note that for a given phase rotating vector, the power of each sample with the index in $\hat{\mathbf{S}}_Y$ or $\hat{\mathbf{S}}_A$ is calculated in that order to calculate the PAPR and find the alternative OFDM signal vector with the minimum PAPR.

The next step is to set γ as the maximum sample power of the first alternative OFDM signal vector. Then γ is compared with each sample power of the second alternative OFDM signal vector in order of indices in $\hat{\mathbf{S}}_Y$ or $\hat{\mathbf{S}}_A$. For instance, γ is compared with the power of $x_{p_k}^{(1)}$ in order of

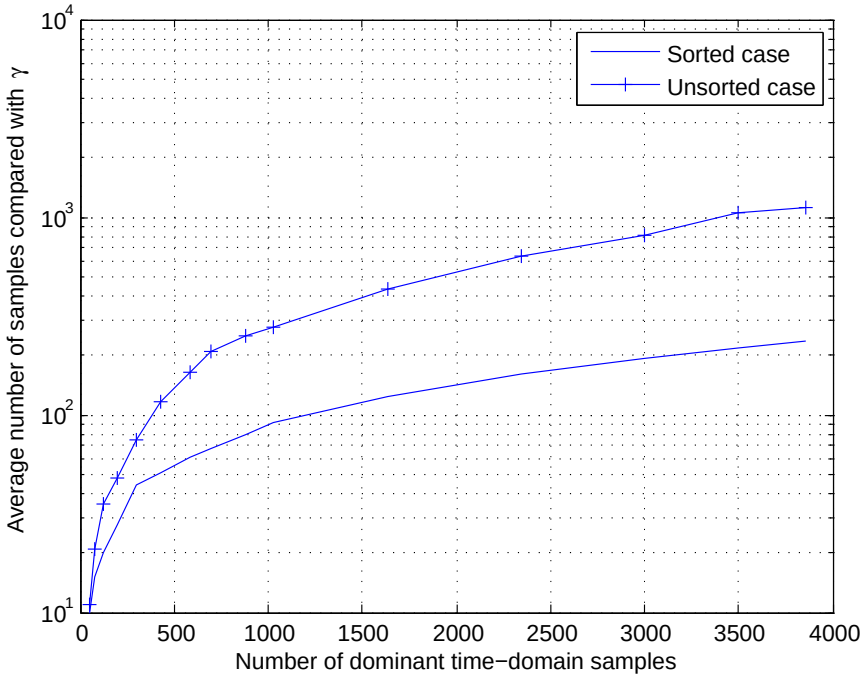

Figure 5.2: Comparison of the average number of compared samples for the sorted and unsorted cases with $L = 4$, $M = 8$, $W = 2$, $N = 1024$, and 16-QAM.

indices in $\hat{\mathbf{S}}_Y$. If the selected sample power is larger than γ, stop calculating the power of the remaining samples and move to the third alternative OFDM signal vector. If all the sample powers are smaller than γ, then γ is updated with the maximum sample power of the second alternative OFDM signal vector and move to the third alternative OFDM signal vector. This procedure is repeated until all alternative OFDM signal vectors are compared with γ and the phase rotating vector giving the final value of γ is selected and the corresponding alternative OFDM signal vector is transmitted.

Since the dominant time-domain samples are rearranged in decreasing

order by their metric values, it is highly probable that samples with large power are firstly dealt with. Let η be the average number of samples compared with γ until a sample with the power bigger than γ is found. Using Monte Carlo simulation, Fig. 5.2 compares η for the sorted $\hat{\mathbf{S}}_Y$ and the unsorted $\mathbf{S}_Y$ for various set size, when $L = 4$, $M = 8$, $W = 2$, $N = 1024$, and 16-QAM are used. It is clear that η for the sorted case is much smaller than that of the unsorted case and therefore, the computational complexity of the proposed scheme can be reduced by sorting the samples without performance degradation.

The procedure of the proposed low-complexity PTS schemes is summarized as follows.

1) An input data vector is divided into M disjoint subblocks and each of them is IFFTed.

2) Determine $\mathbf{S}_Y$ or $\mathbf{S}_A$ in (5.6).

3) If the proposed scheme in Subsection 5.2.1 is only considered, the sample $x_n^{(u)}$ in the set obtained in Step 2) is multiplied with all phase rotating vectors to calculate the PAPR of $\mathbf{x}^{(u)}$ and then go to Step 8). Otherwise, go to Step 4).

4) Sort the elements in $\mathbf{S}_Y$ or $\mathbf{S}_A$ in decreasing order using their corresponding metric values and make the sorted index sets $\hat{\mathbf{S}}_Y$ and $\hat{\mathbf{S}}_A$.

5) Set γ as the maximum sample power of the first alternative OFDM signal vector.

Table 5.1: Computational complexity of the Con-PTS, RC-PTS, and the proposed PTS schemes.

Complexity	Number of real multiplications			
Step	2)	3), 4)	5), 6), 7)	8)
Con-PTS	$4MLNU + 2LNU$			
RC-PTS	$2MLN$	$4KMU$ $+2KU$	0	$4LNM$ $+2LN$
Proposed(Y)	$3MLN$			
Proposed(A)	$2LN$			
Proposed(SY)	$3MLN$	0	$4\eta MU$ $+2\eta U$	$4LNM$ $+2LN$
Proposed(SA)	2LN			

Complexity	Number of real additions			
Step	2)	3), 4)	5), 6), 7)	8)
Con-PTS	$2MLNU + 2LNU(M-1) + 2LNU + U$			
RC-PTS	$LN(M-1)+$ $MLN + LN$	$2KU(M-1)$ $+2KMU$ $+2KU + U$	0	$2LN(M-1)$ $+2LNM$
Proposed(Y)	$LN(M-1)+$ $MLN + LN$			
Proposed(A)	$2LN(M-1)+$ $2LN$			
Proposed(SY)	$2LN(M-1)$	$K \log_2 K$	$2\eta MU+$ $2\eta U(M-1) + \eta U$	$2LN(M-1)$ $+2LNM$
Proposed(SA)	$2LN(M-1)$			

6) Each sample power with index in $\hat{\mathbf{S}}_Y$ or $\hat{\mathbf{S}}_A$ is compared with γ. If a sample power is larger than γ, stop calculating sample power and go to Step 7). Otherwise, γ is updated by the maximum sample power of the second alternative OFDM signal vector and go to Step 7).

7) Repeat Step 6) for all the remaining alternative OFDM signal vectors and then, the phase rotating vector corresponding to the final γ is used to make the optimal OFDM signal vector $\mathbf{x}^{(u_{opt})}$.

8) Transmit the optimal OFDM signal vector $\mathbf{x}^{(u_{opt})}$ with the side information on u_{opt}.

5.2.3. Computational Complexity Analysis

Table 5.1 compares the computational complexity in terms of real multiplications and real additions for the conventional PTS (Con-PTS), RC-PTS, two proposed PTS schemes using $\mathbf{S}_Y$ (Proposed(Y)) and using $\mathbf{S}_A$ (Proposed(A)), and two proposed PTS schemes using $\hat{\mathbf{S}}_Y$ (Proposed(SY)) and using $\hat{\mathbf{S}}_A$ (Proposed(SA)).

When the number of subblocks is fixed, the computational complexity for Step 1) is the same for all PTS schemes, and therefore, only the other steps are considered. In general, one complex multiplication requires four real multiplications and two real additions, and one complex addition requires two real additions. Also, one comparison and one square root operation are equivalent to one real addition and one real multiplication, respectively. The number of selected dominant time-domain samples with each metric is denoted by K and quick sorting algorithm [43] is used at Step 4), which requires $K \log_2 K$ real additions. Note that the average number of samples compared with γ is denoted by η as in Fig 5.2.

It is clear that K is an important factor for the computational complexity of Proposed(Y) and Proposed(A), whereas η is also an important factor for the computational complexity of Proposed(SY) and Proposed(SA). The detailed numerical analysis is given in the following section.

5.3. Simulation Results

Fig. 5.3 compares the PAPR reduction performance of four proposed PTS schemes (Proposed(Y), Proposed(A), Proposed(SY), and Proposed(SA)),

with that of RC-PTS and Con-PTS, when $N = 1024$, $L = 4$, $M = 8$, $W = 2$, and 16-QAM are used. For fair comparison, the same K is used for the proposed low-complexity PTS schemes by adjusting thresholds for each scheme and the corresponding η is determined as $\eta = 76$ for $K = 800$ and $\eta = 92$ for $K = 1100$ from extensive numerical analysis. Fig. 5.3 shows that the PAPR reduction performance of Proposed(SY) and Proposed(SA) is exactly the same as that of Proposed(Y) and Proposed(A), respectively, as expected. For the same K, the proposed PTS schemes show better PAPR reduction performance than RC-PTS scheme. Moreover, $K = 800$ for Proposed(A), $\eta = 76$ ($K = 800$) for Proposed(SA), $K = 1100$ for Proposed(Y), $\eta = 92$ ($K = 1100$) for Proposed(SY), and $K = 1400$ for RC-PTS are needed to show the same PAPR reduction performance as the conventional PTS (Con-PTS).

The computational complexity of the proposed schemes is compared with that of Con-PTS in Fig. 5.4 in terms of relative computational complexity(%) when the PAPR reduction performance is the same as explained in the above. The relative computational complexity of real multiplications for RC-PTS, Proposed(Y), Proposed(A), Proposed(SY), and Proposed(SA) compared with that of Con-PTS are 35.3%, 27.6%, 20.3%, 3.6%, and 2.7%, respectively. Also, the relative computational complexity of real additions shows a similar tendency as the relative computational complexity of real multiplications, which are 33.9%, 28%, 20.7%, 3.4%, and 2.9%. Under the same PAPR reduction performance, Proposed(SA) needs less than 3% of the computational complexity of Con-PTS.

Fig. 5.5 compares the PAPR reduction performance of Con-PTS, RC-PTS, and four proposed PTS schemes with $N = 1024$, $L = 4$, $M = 4$, $W = 4$, and 16-QAM. It is shown that Proposed(Y) needs $K = 120$ to achieve the same PAPR reduction performance as Con-PTS, meanwhile RC-PTS and Proposed(A) need $K = 250$ and $K = 450$, respectively. Proposed(SY) needs $\eta = 24$ with $K = 120$, whereas Proposed(SA) needs $\eta = 55$ with $K = 450$. Using Table 5.1, the relative computational complexity of real multiplications for RC-PTS, Proposed(Y), Proposed(A), Proposed(SY), and Proposed(SA) are calculated as 8.4%, 5.5%, 12.5%, 3.1%, and 3.1%, respectively, and the relative computational complexity of real additions is calculated as 8.3%, 5.1%, 13.1%, 2.6%, and 3.5%, respectively.

5.4. Conclusion

In this chapter, two effective metrics are proposed to select dominant time-domain OFDM signal samples and two low-complexity PTS schemes based on these two metrics are proposed. For more complexity reduction, sorting the selected dominant time-domain samples is proposed. Numerical analysis shows that the proposed PTS schemes can achieve the same PAPR reduction performance as that of the conventional PTS scheme with substantially reduced computational complexity.

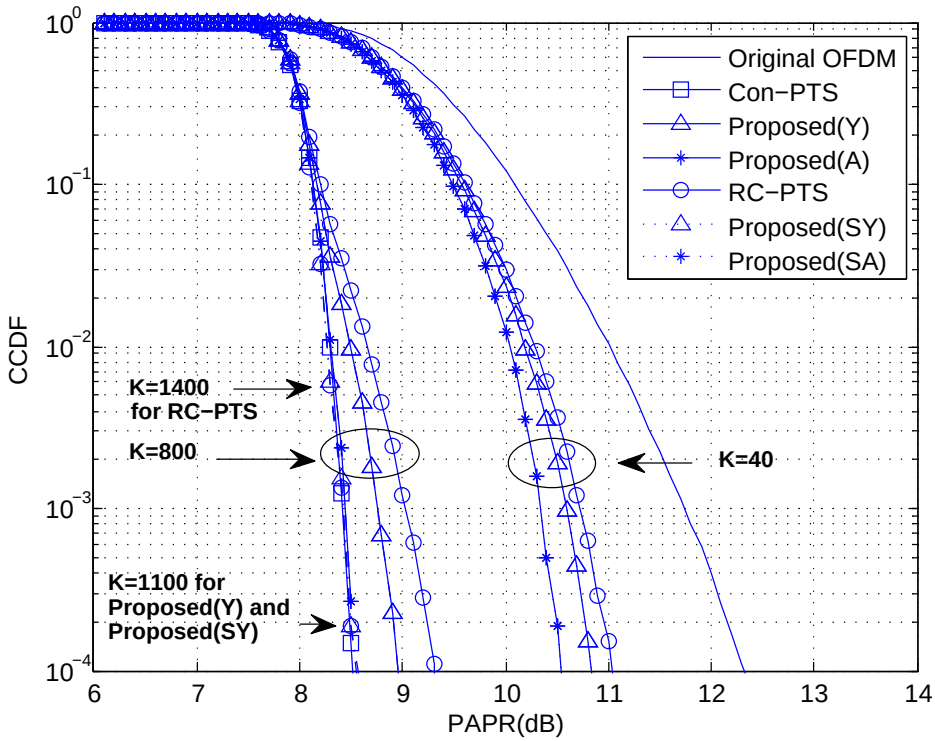

Figure 5.3: Comparison of PAPR reduction performance of Con-PTS, RC-PTS, and four proposed PTS schemes for $N = 1024$, $L = 4$, $M = 8$, $W = 2$, and 16-QAM.

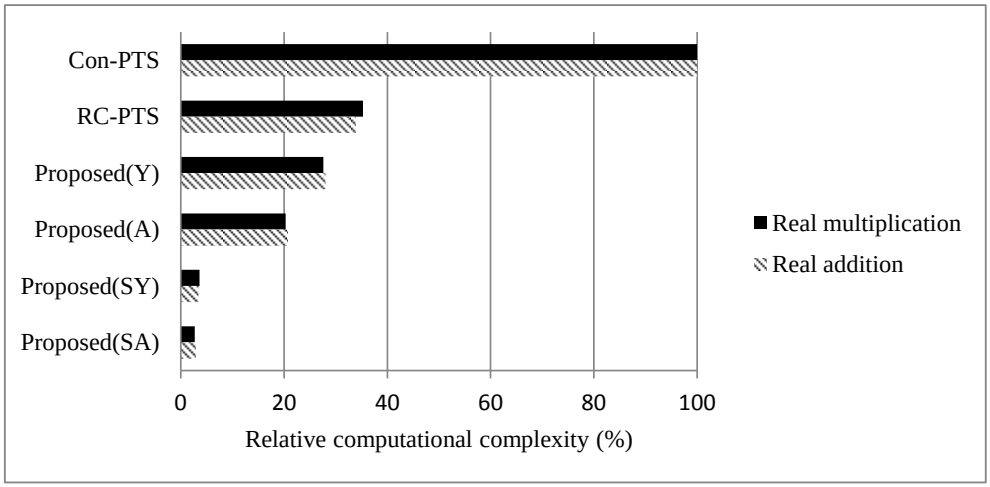

Figure 5.4: Comparison of computational complexity of Con-PTS, RC-PTS, and four proposed PTS schemes under the same PAPR reduction performance for $N = 1024$, $L = 4$, $M = 8$, $W = 2$, and 16-QAM.

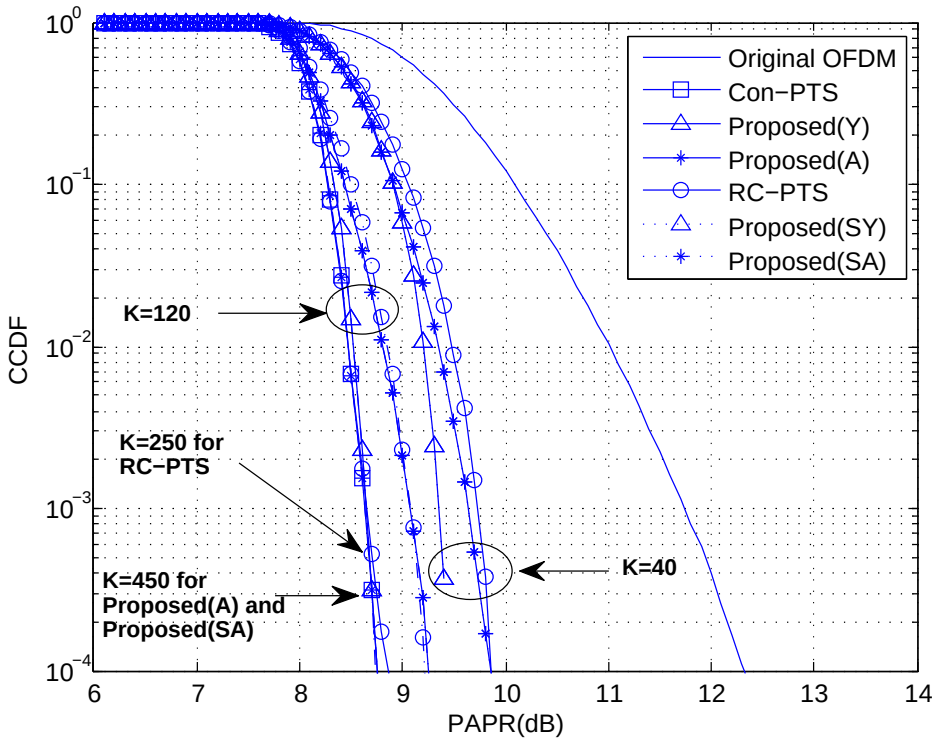

Figure 5.5: Comparison of PAPR reduction performance of Con-PTS, RC-PTS, and four proposed PTS schemes for $N = 1024$, $L = 4$, $M = 4$, $W = 4$, and 16-QAM.

Chapter 6. Low-Complexity PTS Schemes Using OFDM Sample Rotation

6.1. Introduction

The computational complexity of PTS scheme increases exponentially with the number of the subblocks, which comes from many IFFT and PAPR computation of lots of alternative OFDM signal vectors. When the number of IFFTs is fixed, the computational complexity of PTS scheme is determined by generation of many alternative OFDM signal vectors and computation of PAPRs of alternative OFDM signal vectors.

In the RC-PTS, summing the power of the n-th time-domain samples of each subblock is used to find the indices of the dominant time-domain samples exceeding the preset threshold of the alternative OFDM signal vectors. Only the selected dominant time-domain samples are multiplied with the phase rotating vectors to calculate PAPR of each alternative OFDM signal vector, which substantially reduces the computational complexity.

In this chapter, a new selection method of the dominant time-domain samples is proposed by rotating the IFFTed signal samples to the area on which the IFFTed signal sample of the first subblock is located in the signal space. Moreover, the method of pre-exclusion of the phase rotating vectors using the time-domain sample rotation is proposed to reduce

the number of alternative OFDM signal vectors. Numerical results confirm that the proposed PTS schemes show large computational complexity reduction without PAPR degradation.

The rest of this chapter is organized as follows. In Section 6.2, new low-complexity PTS schemes using the time-domain sample rotation and the pre-exclusion of the phase rotating vectors are proposed. In Section 6.3, the computational complexity of the proposed PTS schemes is analyzed and the simulation results are provided. Finally, conclusion is given in Section 6.4.

6.2. New Low-Complexity PTS Schemes

In this section, two method of the computational complexity reduction of PAPR of the PTS schemes are proposed. In Subsection 6.2.1, a new method to select the dominant time-domain samples is proposed to further reduce the computational complexity of PAPR of alternative OFDM signal vectors. Moreover, the number of alternative OFDM signal vectors is reduced by eliminating a subset of phase rotating vectors in Subsection 6.2.2. And using two proposed methods, three new low-complexity PTS schemes are proposed in Subsection 6.2.3.

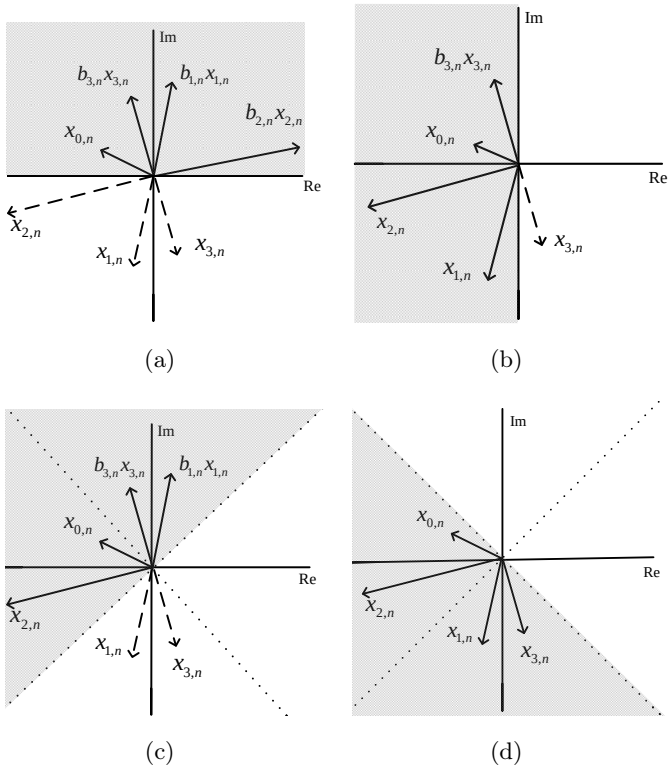

Figure 6.1: The n-th IFFTed signal sample rotation by 180° to the IFFTed signal sample of the first subblock reflecting by (a) real axis (b) imaginary axis (c) real axis with $\pi/4$ rotation (d) imaginary axis with $\pi/4$ rotation for $M = 4$ and $W = 2$.

6.2.1. A New Selection Method of Dominant Time-Domain Samples Using Signal Rotation

Let V_n denote the maximum magnitude of n-th sample among U alternative OFDM signal vectors in the PTS scheme, which is

$$V_n = \max_{u=0}^{U-1} \left| \sum_{m=0}^{M-1} b_{m,n}^{(u)} x_{m,n} \right| = \max_{u=0}^{U-1} \left| x_n^{(u)} \right|, \qquad n = 0, 1, \cdots, N-1 \quad (6.1)$$

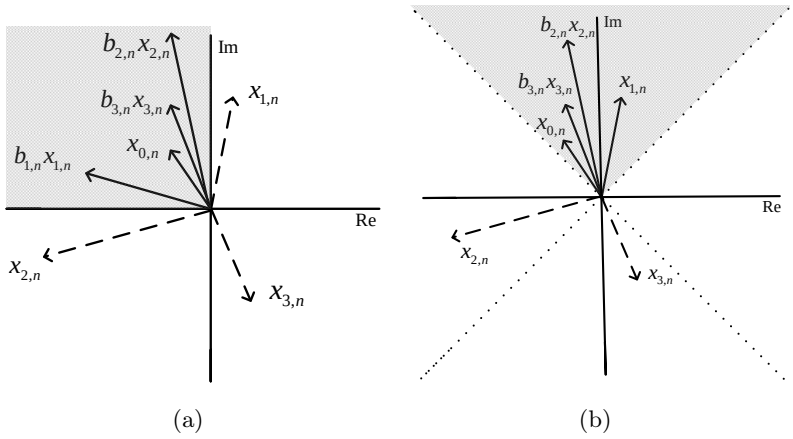

Figure 6.2: The n-th IFFTed signal sample rotation to (a) one quadrant (b) one rotated quadrant by $\pi/4$ for $M = 4$ and $W = 4$.

where $b_{m,n}^{(u)}$ and the metric V_n constitute the n-th phase rotating vector $\mathbf{b}_n^{(u)} = [b_{0,n}^{(u)}, b_{1,n}^{(u)}, \cdots, b_{M-1,n}^{(u)}]$ and $\mathbf{V} = [V_0, V_1, \cdots, V_{N-1}]$, respectively. For a preset threshold γ, the index set of the dominant time-domain samples is given as

$$\mathbf{S}_V = \{n \mid V_n \geq \gamma, \quad 0 \leq n \leq N-1\}. \tag{6.2}$$

Using only the selected dominant time-domain samples with indices in $\mathbf{S}_V$ instead of all time-domain samples, we calculate the PAPRs of all alternative OFDM signal vectors. However, V_n needs full search over all phase rotating vectors, which requires $U = W^{M-1}$ searches.

Thus, in this subsection, we propose a new metric for $\mathbf{S}_V$ using time-domain signal sample rotation with significantly less computational complexity. The n-th IFFTed signal samples of subblocks are rotated to the

area on which the IFFTed signal sample $x_{0,n}$ of the first subblock is located in the signal space to approximately find the maximum magnitude of the n-th time-domain sample. Fig. 6.1 shows four different types of the n-th IFFTed signal sample rotation of each subblock in the signal space for $M = 4$ and $W = 2$. In Fig. 6.1(a), the n-th IFFTed signal samples of subblocks are rotated to the first and the second quadrants reflecting them by the real axis, because $x_{0,n}$ is located in the second quadrant. In Fig. 6.1(b), the n-th IFFTed signal samples of subblock are rotated to the second and the third quadrants reflecting them by the imaginary axis, where $x_{0,n}$ is located. The axes of real and imaginary in Figs. 6.1(c) and 6.1(d) are rotated by $\pi/4$. And the IFFTed signal samples of subblocks are rotated by altered axes as the same manner of Figs. 6.1(a) and 6.1(b).

Fig. 6.2 shows two different types of the n-th IFFTed signal sample rotation by $\pm 90^\circ$ and 180° in the signal space for $M = 4$ and $W = 4$ to approximately find the maximum magnitude of the n-th time-domain sample. It is possible to rotate IFFTed signal samples to the quadrant where the IFFTed signal sample $x_{0,n}$ of the first subblock is located because of $W = 4$.

Using Fig. 6.1 or Fig. 6.2, we have the C alternative time-domain samples at the n-th position given as $[x_n^{(u_n,0)}, x_n^{(u_n,1)}, \cdots, x_n^{(u_n,C-1)}]$, where $u_n, n = 0, 1, \cdots, N-1$, is the selected indices among U alternative OFDM signal vectors with $C = 4$ in Fig. 6.1 and $C = 2$ in Fig. 6.2. Therefore, a new metric P_n to find $\mathbf{S}_V$ instead of the true maximum magnitude V_n is

proposed as

$$P_n = \max_{c=0}^{C-1} |x_n^{(u_n,c)}|. \tag{6.3}$$

Let $\mathbf{S}_P$ be the index set of the dominant time-domain samples defined as

$$\mathbf{S}_P = \{n \mid P_n \geq \gamma_p, \quad 0 \leq n \leq N-1\} \tag{6.4}$$

where γ_p is the preset threshold for P_n. Then only the n-th samples of subblocks with indices $n \in \mathbf{S}_P$ are used for calculation of PAPR values of alternative OFDM signal vectors. In fact, P_n is considered as an approximation of V_n, which gives us the substantial reduction of the computational complexity.

Now, we can compute the estimation error of V_n by P_n. The normalized mean square error (NMSE) defined by

$$NMSE = \frac{1}{N} \sum_{n=0}^{N-1} \frac{(P_n - V_n)^2}{E[P_n]E[V_n]}. \tag{6.5}$$

Table 6.1 lists the NMSE for the metric P_n (or Q_n) and V_n with $M = 4$, $L = 4$, $C = 4$ (for $W = 2$), $C = 2$ (for $W = 4$), and $N = 1024$. The NMSE of P_n and V_n is much lower than that of Q_n and V_n regardless of M and W, which means that P_n can be more closely approximated to V_n compared to Q_n.

6.2.2. Pre-Exclusion of Phase Rotating Vectors

The proposed low-complexity PTS scheme can also reduce alternative OFDM signal vectors by eliminating some phase rotating vectors. The eliminated phase rotating vectors are called pre-excluded phase rotating

Table 6.1: NMSE for the metrics and V_n in case of $M = 4$, $L = 4$, and $N = 1024$ with different W.

Number of subblocks	$W = 2(C = 4)$		$W = 4(C = 2)$	
	P_n	Q_n	P_n	Q_n
4	1.4×10^{-5}	5.4×10^{-3}	1.0×10^{-4}	6.7×10^{-3}
6	4.0×10^{-5}	6.9×10^{-3}	1.4×10^{-4}	8.2×10^{-3}
8	6.6×10^{-5}	7.8×10^{-3}	1.6×10^{-4}	9.1×10^{-3}

vectors. Using Fig. 6.1 or Fig. 6.2, we obtain the C phase rotating vectors as $[\mathbf{b}_n^{(u_n,0)}, \mathbf{b}_n^{(u_n,1)}, \cdots, \mathbf{b}_n^{(u_n,C-1)}]$, which are the phase rotating vectors to approximately find the maximum magnitude of the n-th time-domain sample.

Let $\mathbf{E}_P$ be the set of the pre-excluded phase rotating vectors defined by

$$\mathbf{E}_P = \{\mathbf{b}_n^{(u_n,c)} \mid |x_n^{(u_n,c)}| \geq \gamma_v, \quad 0 \leq c \leq C-1, \quad 0 \leq n \leq N-1\} \quad (6.6)$$

where γ_v is the preset threshold to find the pre-excluded phase rotating vectors, which is excluded from U phase rotating vectors.

Therefore, U_s survived phase rotating vectors to generate alternative OFDM signal vectors is obtained by removing pre-excluded phase rotating vectors from U phase rotating vectors, that is,

$$U_s = U - U_p \quad (6.7)$$

where U_p is the number of pre-excluded phase rotating vectors given as $U_p = |\mathbf{E}_P|$.

Table 6.2: An example of $\mathbf{x}_m$ in the proposed PTS using dominant time-domain samples for $M = 4$ and $N = 8$.

$x_{m,n}$	$x_{m,0}$	$x_{m,1}$	$x_{m,2}$	$x_{m,3}$	$x_{m,4}$	$x_{m,5}$	$x_{m,6}$	$x_{m,7}$
$\mathbf{x}_0$	0	0	0	$0.21 - j0.09$	0.25	$0.21 + j0.09$	0	0
$\mathbf{x}_1$	0	0	0	$-0.09 - j0.21$	0.25	$-0.09 + j0.21$	0	0
$\mathbf{x}_2$	0	0	0	$0.21 - j0.09$	-0.25	$0.21 + j0.09$	0	0
$\mathbf{x}_3$	0	0	0	$0.09 - j0.04$	0.25	$0.09 + j0.04$	0	0

6.2.3. The Proposed Low-Complexity PTS Schemes

Using the two proposed methods in Subsections 6.2.1 and 6.2.2, the optimal phase rotating vector $\mathbf{b}^{(u_{opt})}$ is obtained as

$$u_{opt} = \arg \min_{u=0}^{U_s-1} \frac{\max_{n \in \mathbf{S}_P} \left| \sum_{m=0}^{M-1} b_m^{(u)} x_{m,n} \right|^2}{E[|x_n|^2]}. \tag{6.8}$$

That is, selecting $\mathbf{x}^{(u_{opt})}$ by using (6.8) adopts two proposed methods, which are selection of the dominant time-domain samples using $\mathbf{S}_P$ in Subsection 6.2.1 and the reduction of the U alternative OFDM signal vectors by using pre-excluded phase rotating vectors in Subsection 6.2.2. Now, we propose three low-complexity PTS schemes using two proposed methods in the previous subsections, that is, a PTS scheme using the dominant time-domain samples (PS-PTS), a PTS scheme using pre-excluded phase rotating vectors (PE-PTS), and a PTS scheme using combination of two proposed methods (PC-PTS). Fig. 6.3 shows the block diagram of the proposed PTS scheme to find $\mathbf{x}^{(u_{opt})}$ by using (6.8).

Using the example of the conventional PTS scheme with $M = 4$,

$W = 2$, and $N = 8$ in Section 3.3, we can give an example of the proposed schemes. Considering Fig. 6.1, we can obtain P_n for N samples as $[0.25, 0.43, 0.56, 0.60, 0.75, 0.60, 0.56, 0.43]$. When $\gamma_p = 0.6$, we have the index set $\mathbf{S}_P = \{3, 4, 5\}$. In order to reduce the computational complexity, we can select the dominant time-domain samples as $\mathbf{x}_m = [0, 0, 0, x_{m,3}, x_{m,4}, x_{m,5}, 0, 0]$ from Table 3.1 by a proposed metric, which is shown in Table 6.2. Also, $\mathbf{b}^{(0)}$ and $\mathbf{b}^{(5)}$ phase rotating vectors are used to make the three largest P_n values. Then we can make three low-complexity PTS schemes as follows:

1) The samples $x_{m,3}$ and $x_{m,5}$ are combined with U phase rotating vectors to calculate PAPR of each alternative OFDM signal vector (PS-PTS).

2) If $\mathbf{b}^{(0)}$ and $\mathbf{b}^{(5)}$ phase rotating vectors are survived by using signal rotation, 8 alternative OFDM signal vectors are reduced to 2 alternative OFDM signal vectors by pre-excluding the phase rotating vectors (PE-PTS).

3) The samples $x_{m,3}$ and $x_{m,5}$ are only combined with $\mathbf{b}^{(1)}$ and $\mathbf{b}^{(5)}$ to calculate PAPR of each alternative OFDM signal vector (PC-PTS).

The thresholds γ_p and γ_v can be determined differently, because selecting many dominant time-domain samples with γ_p may results in elimination of too many phase rotating vectors. Fig. 6.4 shows the number of selected dominant time-domain samples using $\mathbf{S}_P$ with different γ_p versus the average number of survived phase rotating vectors for $N = 1024$, $L = 4$, and 16-QAM with 10^5 iterations. It is shown that selecting more than 280 and 500 dominant time-domain samples by γ_p results in elim-

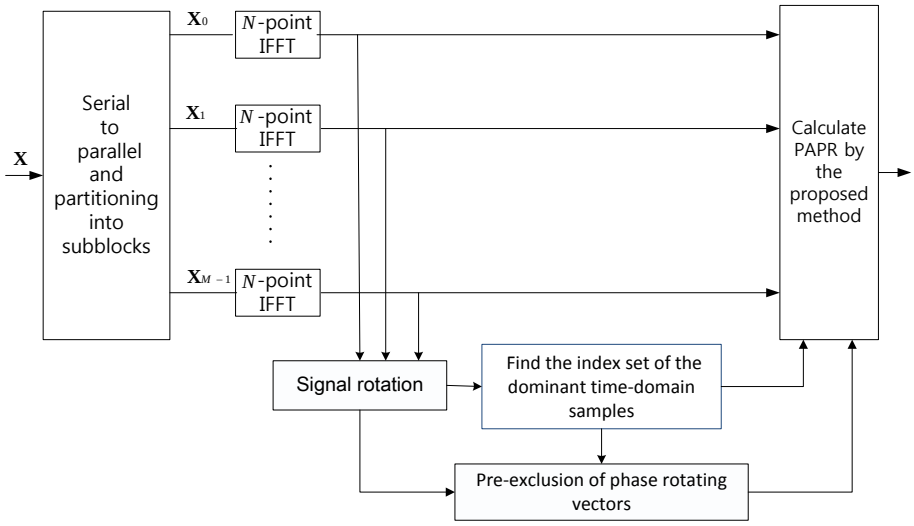

Figure 6.3: The block diagram of the proposed PTS scheme.

inating almost all the phase rotating vectors for $M = 4$, $W = 4$, and $M = 8$, $W = 2$, respectively.

The procedures of the proposed low-complexity PTS schemes are summarized as follows:

1. PS-PTS scheme:

   (a) An input data vector is divided into M disjoint subblocks, which are IFFTed.

   (b) In order to approximate the maximum magnitude of $x_n^{(u)}$ by using Fig. 6.1 or Fig. 6.2, calculate P_n.

   (c) Find the index set $\mathbf{S}_P$ with γ_p.

   (d) Only the dominant time-domain samples in the set $\mathbf{S}_P$ are used to calculate the PAPR of $\mathbf{x}^{(u)}$ and select the optimal phase rotating vector $\mathbf{b}^{(u_{opt})}$.

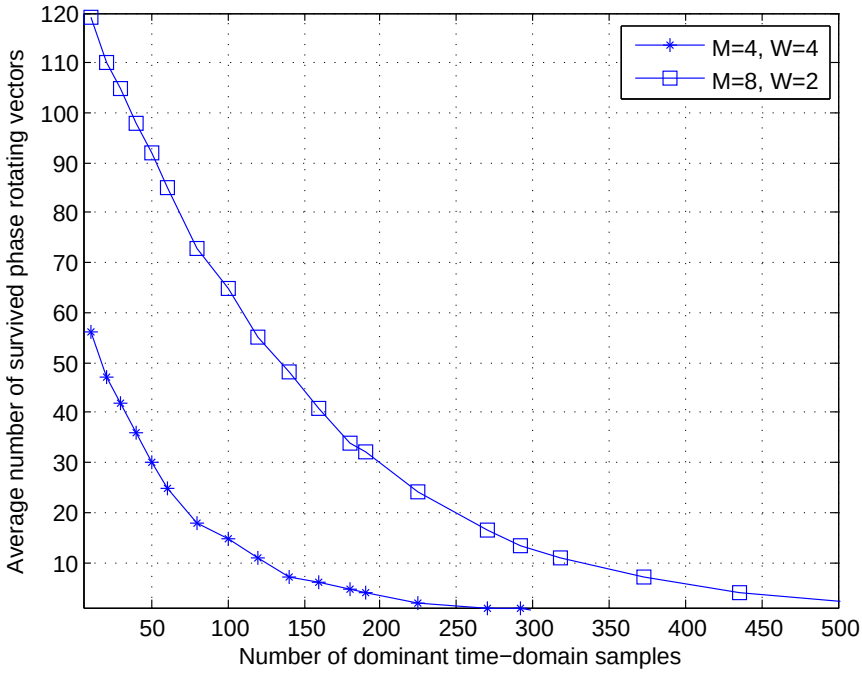

Figure 6.4: The number of selected dominant time-domain samples versus the average number of survived phase rotating vectors for $N = 1024$, $L = 4$, and 16-QAM.

(e) Generate $\mathbf{x}^{(u_{opt})}$ using $\mathbf{b}^{(u_{opt})}$ and transmit it.

2. PE-PTS scheme:

(a) An input data vector is divided into M disjoint subblocks, which are IFFTed.

(b) By computing the approximated maximum magnitude of $x_n^{(u)}$ using Fig. 6.1 or Fig. 6.2, find the set of pre-excluded phase rotating vectors using (6.6).

(c) Using (6.6) and (6.7), the U_s survived phase rotating vectors are obtained.

(d) Among U_s alternative OFDM signal vectors, find $\mathbf{x}^{(u_{opt})}$ and transmit it.

3. PC-PTS scheme:

(a) An input data vector is divided into M disjoint subblocks, which are IFFTed.

(b) By computing the approximated maximum magnitude of $x_n^{(u)}$ using Fig. 6.1 or Fig. 6.2;

b-1) Find the set of pre-excluded phase rotating vectors using (6.6) and the U_s survived phase rotating vectors are obtained from (6.6) and (6.7).

b-2) Calculate P_n and find the index set $\mathbf{S}_P$ with γ_p.

(c) Select the optimal phase rotating vector $\mathbf{b}^{(u_{opt})}$ using (6.8).

(d) Generate $\mathbf{x}^{(u_{opt})}$ using $\mathbf{b}^{(u_{opt})}$ and transmit it.

6.3. Computational Complexity and Simulation Results

6.3.1. Computational Complexity

In this subsection, we compare the computational complexity of the conventional PTS, RC-PTS, and three proposed PTS schemes, which are PS-PTS, PE-PTS, and PC-PTS for $M = 8$, $L = 4$, $W = 2$, $N = 1024$, and $C = 4$. Since the computational complexity of the complex additions shows the similar tendency, only the complex multiplication for generating alternative OFDM signal vectors is considered. For a fair comparison, the

Table 6.3: Computational complexity for the conventional PTS, RC-PTS, and the proposed schemes with $M = 8$, $L = 4$, $W = 2$, $N = 1024$.

Schemes	Number of complex multiplications	PAPR(10^{-4})
Conventional	$LNU = 524288(100\%)$	$8.4dB$
RC-PTS	$MLN + p_\alpha LNU = 69468.16(13.3\%)$	$10dB$
PS-PTS	$CLN + p_\alpha LNU = 53084.16(10.1\%)$	$8.4dB$
PE-PTS	$CLN + LNU_s = 86016(16.4\%)$	$8.4dB$
PC-PTS	$CLN + p_\alpha LNU_s = 6021.12(1.1\%)$	$8.4dB$

average probability p_α of the selected dominant time-domain samples is set to 0.07 and U_s is set to 17 for the same PAPR reduction performance as the conventional one, which will be shown in the next subsection.

Note that while RC-PTS needs MLN complex multiplications to make the metric Q_n [38], the proposed PTS schemes need CLN complex multiplications. Table 6.3 shows that, compared with the number of complex multiplications required by the conventional PTS, the PC-PTS requires the lowest computational complexity of 1.1% with PAPR $8.4dB$, which gives the same PAPR reduction performance as the conventional PTS, whereas the RC-PTS requires the computational complexity of 13.3% with PAPR $10dB$. Although the computational complexity of PE-PTS is higher than that of RC-PTS, PE-PTS is very useful in that the number of alternative OFDM signal vectors can be reduced by pre-excluding phase rotating vectors. Thus, in general, the PE-PTS can be combined with other low-complexity PTS schemes using the dominant time-domain samples including the conventional PTS.

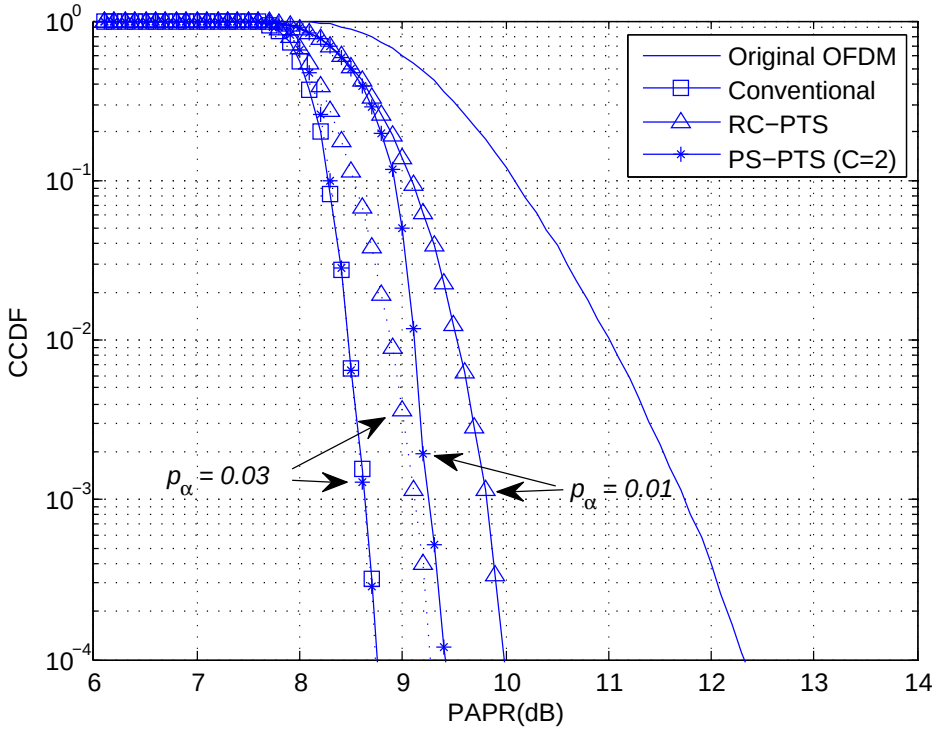

Figure 6.5: Comparison of PAPR reduction performance of the conventional PTS, RC-PTS, and PS-PTS schemes with $N = 1024$, $L = 4$, $M = 4$, $C = 2$, $W = 4$, 16-QAM, and $p_\alpha = 0.01, 0.03$.

6.3.2. Simulation Results

Fig. 6.5 compares the PAPR reduction performance of PS-PTS with RC-PTS and the conventional PTS, where $N = 1024$, $L = 4$, $M = 4$, $C = 2$, $W = 4$, and 16-QAM are used. The p_α is set to 0.01 and 0.03 for different γ_p. It is shown that 3% of time-domain samples of PS-PTS is sufficient to perform the same PAPR reduction performance as the conventional PTS, whereas 3% of time-domain samples of RC-PTS degrades the PAPR reduction performance by $0.4dB$.

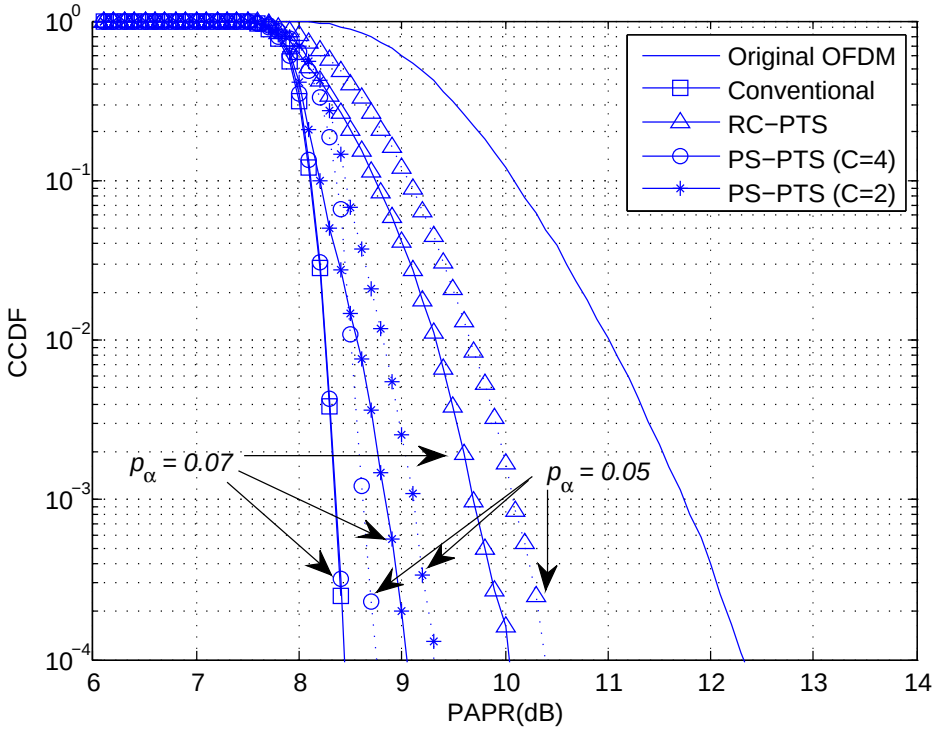

Figure 6.6: Comparison of PAPR reduction performance of the conventional PTS, RC-PTS, and PS-PTS schemes with different C in case of $N = 1024$, $L = 4$, $M = 8$, $W = 2$, 16-QAM, and $p_\alpha = 0.05, 0.07$.

Fig. 6.6 shows that the PAPR reduction performance of the conventional PTS, RC-PTS, and PS-PTS schemes with different C for $N = 1024$, $L = 4$, $M = 8$, $W = 2$, 16-QAM, and $p_\alpha = 0.05, 0.07$. Two PS-PTS schemes are simulated, which are PS-PTS with $C = 2$ using Fig. 6.1(a) and Fig. 6.1(b), and PS-PTS with $C = 4$ using all four cases in Fig. 6.1. It is shown that PS-PTS with $C = 4$ shows the same PAPR reduction performance as the conventional one with only 7% of time-domain samples. Also, the PAPR reduction performance of two proposed PTS schemes

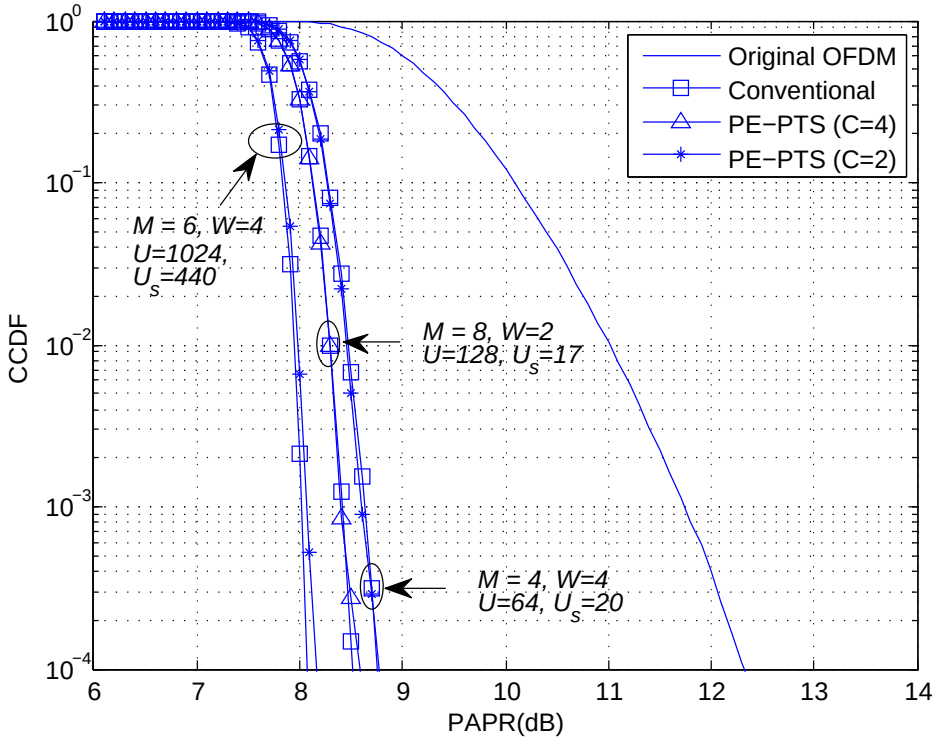

Figure 6.7: Comparison of PAPR reduction performance of the conventional PTS and PE-PTS schemes with $N = 1024$, $L = 4$, 16-QAM, $M = 4, 6, 8$, and $W = 2, 4$.

shows better than that of RC-PTS.

Fig. 6.7 demonstrates the PAPR reduction performance of the conventional PTS and PE-PTS with $N = 1024$, $L = 4$, 16-QAM, $M = 4, 6, 8$, and $W = 2, 4$. The conventional PTS needs $U = 128$ alternative OFDM signal vectors with $M = 8$ and $W = 2$, meanwhile the PE-PTS needs only 17 alternative OFDM signal vectors. Also, when the conventional PTS needs $U = 64$ with $M = 4$ and $W = 4$, and $U = 1024$ with $M = 6$ and $W = 4$, the PE-PTS needs only $U_s = 20$ and $U_s = 440$, respectively.

Fig. 6.8 shows the PAPR reduction performance of the PC-PTS with

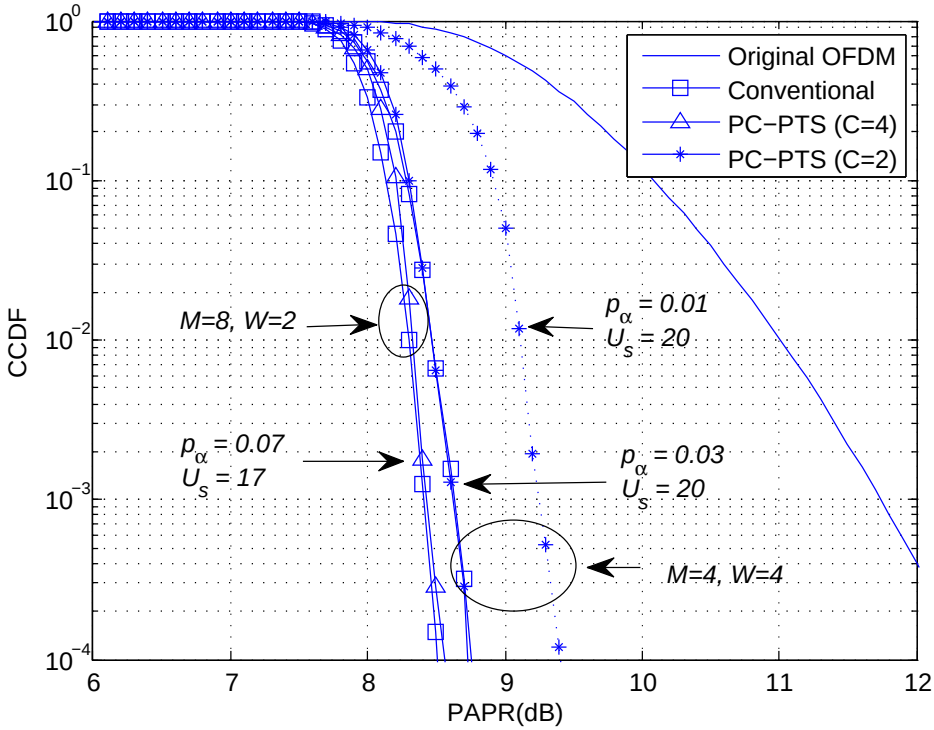

Figure 6.8: Comparison of PAPR reduction performance of the conventional PTS and two PC-PTS schemes with $N = 1024$, $L = 4$, 16-QAM, $M = 4, 8$, and $W = 2, 4$.

$N = 1024$, $L = 4$, 16-QAM, $M = 4, 8$, and $W = 2, 4$. When U_s is used as the same U_s in Fig. 6.7, the PAPR reduction performance of PC-PTS with $p_\alpha = 0.07$ is the same as that of the conventional PTS for $M = 8$ and $W = 2$, but its computational complexity is substantially reduced by using small number of alternative OFDM signal vectors. For $M = 4$ and $W = 4$, it is shown that the PAPR reduction performance of the PC-PTS with substantially reduced $U_s = 20$ alternative OFDM signal vectors is the same as that of the PS-PTS.

Fig. 6.9 compares the PAPR reduction performance of PS-PTS with

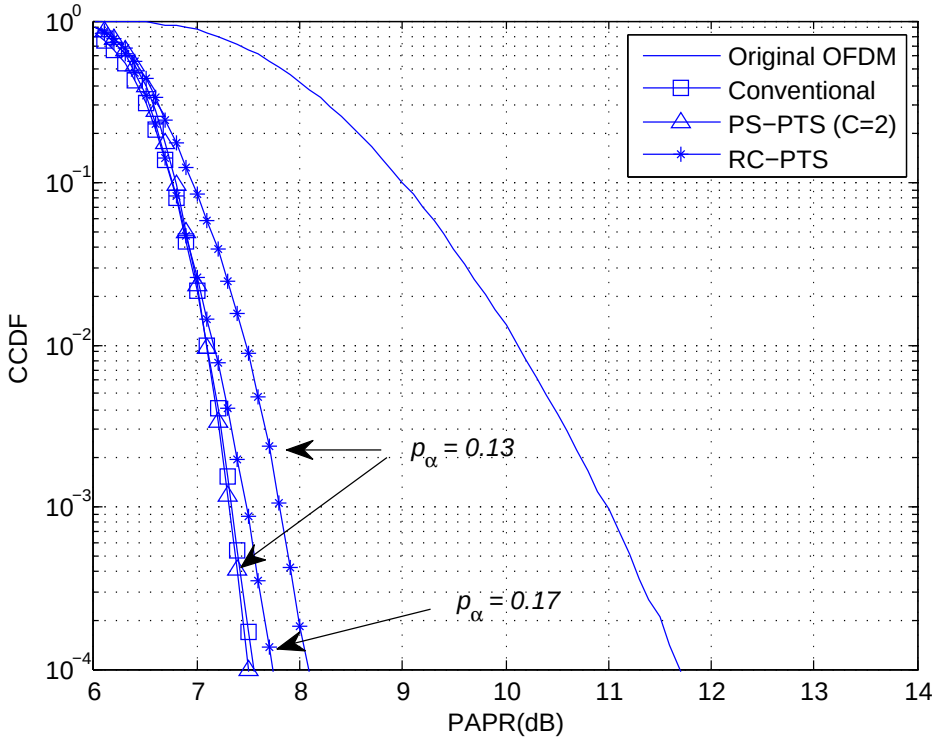

Figure 6.9: Comparison of PAPR reduction performance of the conventional PTS, RC-PTS, and PS-PTS schemes with $N = 128$, $L = 4$, $M = 4$, $C = 2$, $W = 4$, 16-QAM, and $p_\alpha = 0.13, 0.17$.

RC-PTS and the conventional PTS, where $N = 128$, $L = 4$, $M = 4$, $C = 2$, $W = 4$, and 16-QAM are used. The p_α is set to 0.13 and 0.17 for different γ_p. It is shown that 13% of time-domain samples of PS-PTS is sufficient to perform almost the same PAPR reduction performance as the conventional PTS.

Fig. 6.10 shows the PAPR reduction performance of the conventional PTS and PE-PTS with $N = 128$, $L = 4$, 16-QAM, $M = 4, 8$, and $W = 2, 4$. The PE-PTS for $M = 8$ and $W = 2$ needs only 35 alternative OFDM

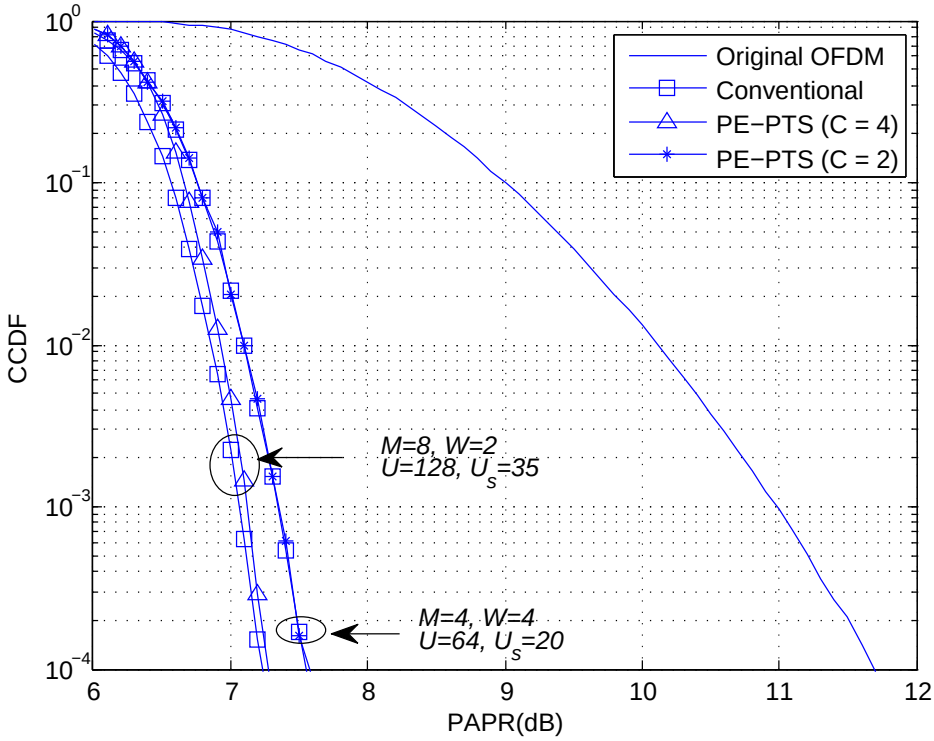

Figure 6.10: Comparison of PAPR reduction performance of the conventional PTS and PE-PTS schemes with $N = 128$, $L = 4$, 16-QAM, $M = 4, 8$, and $W = 2, 4$.

signal vectors among $U = 128$ alternative OFDM signal vectors. Also, when the conventional PTS needs $U = 64$ with $M = 4$ and $W = 4$, the PE-PTS needs only $U_s = 20$.

6.4. Conclusion

In this chapter, three proposed PTS schemes are introduced to reduce the computational complexity by using simple OFDM signal rotation and pre-exclusion of the phase rotating vectors. The computational complex-

ity for the computation of PAPRs of alternative OFDM signal vectors is reduced by using the selected dominant time-domain samples by a new simple proposed metric. Also, the number of alternative OFDM signal vectors is reduced by pre-excluding the phase rotating vectors. Numerical analysis shows that the proposed PTS schemes achieve the same PAPR reduction performance as that of the conventional PTS scheme with the large computational complexity reduction.

Chapter 7. Conclusions

This dissertation proposes several research results on the PAPR reduction schemes for the OFDM systems. Although OFDM has bandwidth efficiency and robustness in the fading channel, it has high PAPR, which degrades power efficiency of the nonlinear HPA at the transmitter. Among many PAPR reduction schemes, the PTS scheme can transmit an OFDM signal without signal distortion, but generating many alternative OFDM signal vectors requires the large computational complexity and causes the rate loss in the PTS scheme. In this dissertation, we propose several PTS schemes to reduce the computational complexity.

In Chapter 4, a new two-step search algorithm for PTS scheme is proposed to reduce the computational complexity. In the first step, sequences with good correlation property such as Kasami and quaternary sequences are used as the initial phase vectors. In the second step, by using the initial phase vectors, local search is performed for further searching the phase rotating vectors with very low computational complexity. Numerical analysis shows that the proposed PTS scheme can achieve almost the same PAPR reduction performance as the conventional PTS scheme with much lower computational complexity than other low-complexity PTS schemes.

In Chapter 5, it is proposed that the PAPR values of alternative OFDM signal vectors are approximately computed based on the dominant time-

domain samples selected by using a simple metric. In this chapter, two new effective metrics for selecting the dominant time-domain samples are proposed for the low-complexity PTS scheme. For further lowering the computational complexity, two low-complexity PTS schemes are proposed by sorting the dominant time-domain samples in decreasing order by their metric values. Simulation results confirm that the proposed PTS schemes show identical PAPR reduction performance with substantially reduced computational complexity, compared to the conventional PTS scheme.

In Chapter 6, three proposed PTS schemes are introduced to reduce the computational complexity by using simple OFDM signal rotation and pre-exclusion of the phase rotating vectors. A new selection method of the dominant time-domain samples is proposed by rotating the IFFTed signal samples to the area on which the IFFTed signal sample of the first subblock is located in the signal space. The computational complexity for the computation of PAPRs of alternative OFDM signal vectors is reduced by using the selected dominant time-domain samples by a new simple proposed metric. Also, the number of alternative OFDM signal vectors is reduced by pre-excluding the phase rotating vectors. Numerical results confirm that the proposed PTS schemes show large computational complexity reduction without PAPR degradation.

Bibliography

[1] R. W. Chang and R. A. Gibby, "A theoretical study of performance of an orthogonal multiplexing data transmission scheme," *IEEE Trans. Commun.*, vol. COM-16, no. 4, Aug. 1968.

[2] IEEE Standard for Information Technoloy-Telecommunications and Information Exchange Between Systems-Local and Metropolitan Area Networks-Specific Requirements Part II :Wireless LAN Medium Access Control (MAC) and Physical Layer (PHY) Specifications Amendment 4: Further Higher Data Rate Extension in the 2.4 GHz Band, IEEE Standard 802.11g–2003, Jun. 2003.

[3] V. Tarokh and H. Jafarkhani, "On the computation and reduction of the peak-to-average power ratio in multicarrier communications," *IEEE Trans. Commun.,* vol. 48, no. 1, pp. 37–44, Jan. 2000.

[4] R. Gross and D. Veeneman, "Clipping distortion in DMT ADSL systems." *Electron. Lett.,* vol. 29, no. 24, pp. 2080–2081, Nov. 1993.

[5] J. Tellado and J. M. Cioffi, *Multicarrier Modulation with Low PAR: Appication to DSL and Wireless.* Boston, MA: Kluwer Academic Publisher, 2000.

[6] R. W. Bäuml, R. F. H. Fischer, and J. B. Huber, "Reducing the peak-to-average power ratio of multicarrier modulation by selected mapping," *Electron. Lett.*, vol. 32, no. 22, pp. 2056-2057, Oct. 1996.

[7] S. H. Müller, R. W. Bäuml, R. F. H. Fischer, and J. B. Huber, "OFDM with reduced peak-to-average power ratio by multiple signal representation," *Ann. Telecommun.*, vol. 52, no. 1-2, pp. 58-67, Feb. 1997.

[8] B. S. Krongold and D. L. Jones, "PAR reduction in OFDM via active constellation extension," *IEEE Trans. Broadcast.*, vol. 49, no. 3, pp. 258–268, Sep. 2002.

[9] X. Wang, T. T. Tjhung, and C. S. Ng, "Reduction of peak-to-average power ratio of OFDM system using a companding technique," *IEEE Trans. Broadcast.,* vol. 45, no. 3, pp. 303–307, Sep. 1999.

[10] X. Huang, J. Lu, J. Zheng, K. B. Letaief, and J. Gu, "Companding transform for reduction in peak-to-average power ratio of OFDM signals," *IEEE Trans. Wirelss Commun.,* vol. 3, no. 6, pp. 2030–2039, Nov. 2004.

[11] A. M. Saleh, "Frequency-independent and frequency-dependent nonlinear models of TWT amplifiers," *IEEE Trans. Commun.,* vol. 29, no.11, pp. 1715–1720, Nov. 1981.

[12] C. Rapp, "Effects of HPA nonlinearity on a 4-DPSK/OFDM signal for a digital sound broadcasting system," in *Proc. Sixth International*

Conference on Digital Processing of Signals in Communications, Sep. 1991, vol. 1, pp. 193–197, Leicestershire, UK.

[13] V. Bohara and S.H. Ting, "Theoretical analysis of OFDM signals in nonlinear polynomial models," *in Proc. IEEE Int. Conf. Inf, Commun. Signal precess.,* 2007, pp. 1–5.

[14] J. Palicot and Y. Louët, "Power ratio definitions and analysis in single carrier modulation," EUSIPCO, Antalya, Turkey, Sep. 2005.

[15] R. van Nee and A. de Wild, "Reducing the peak-to-average power ratio of OFDM," *in Proc. IEEE Vehicular Technology Conf. (VTC'98),* May. 1998, vol. 3, pp. 2072–2076.

[16] S. Q. Wei, D. L. Goeckel, and P. E. Kelly, "A modern extreme value theory approach to calculating the distribution of the peak-to-average power ratio in OFDM systems," *in Proc. IEEE Int. Conf. Commun.(ICC),* pp. 1686–1690, Apr. 2004.

[17] H. Ochiai and H. Imai, "On the distribution of the peak to average power ratio in OFDM signals," *IEEE Trans. Commun.,* vol. 49, no. 2, pp. 282–289, Feb. 2001.

[18] J. Armstrong, "Peak-to-average power reduction for OFDM by repeated clipping and frequency domain filtering," *Electron. Lett.,* vol. 38, no. 5, pp. 246–247, Feb. 2002.

[19] S. Kimura, T. Nakamura, M. Saito, and M. Okada, "PAR reduction for OFDM signals based on deep clipping," *3rd International*

Symposium on Communications, Control and Signal Processing, pp. 911–916, Mar. 2008.

[20] S.-J. Heo, H.-S. Noh, J.-S. No, and D.-J. Shin, "A modified SLM scheme with low complexity for PAPR reduction of OFDM systems," *IEEE Trans. Broadcast.*, vol. 53, no. 4, pp. 804–808, Dec. 2007.

[21] H.-B. Jeon, K.-H. Kim, J.-S. No, and D.-J. Shin, "Bit-based SLM schemes for PAPR reduction in QAM modulated OFDM signals," *IEEE Trans. Broadcast.*, vol. 55, no. 3, pp. 679–685, Sep. 2009.

[22] D.-W. Lim, S.-J. Heo, and J.-S. No, "On the phase sequence set of SLM OFDM scheme for a crest factor reduction," *IEEE Trans. Signal Process.*, vol. 54, no. 5, pp. 1931–1935, May 2006.

[23] S. G. Kang, J. G. Kim, and E. K. Joo, "A noble subblock partition scheme for partial transmit sequence OFDM," *IEEE Trans. Broadcast.,* vol. 45, no. 3, pp. 333–338, Sep. 1999.

[24] L. Guan, T. Jiang, D. Qu, and Y. Zhou, "Joint channel estimation and PTS to reduce peak-to-average-power ratio in OFDM systems without side information," *IEEE Signal Process. Lett.,* vol. 17, no. 10, pp. 883–886, Oct. 2010.

[25] A. D. S. Jayalath and C. Tellambura, "SLM and PTS peak-power reduction of OFDM signals without side information," *IEEE Trans. Wirelss Commun.,* vol. 4, no. 5, pp. 2006–2013, Sep. 2005.

[26] L. Yang, K. K. Soo, S. Q. Li, and Y. M. Siu, "PAPR reduction using low complexity PTS to construct of OFDM signals without side information," *IEEE Trans. Broadcast.,* vol. 57, no. 2, pp. 284–290, Jun. 2011.

[27] D.-W. Lim, S.-J. Heo, J.-S. No, and H. Chung, "A new PTS OFDM scheme with low complexity for PAPR reduction," *IEEE Trans. Broadcast.*, vol. 52, no. 1, pp. 77–82, Mar. 2006.

[28] L. J. Cimini and N. R. Sollenberger, "Peak-to-average power ratio reduction of an OFDM signal using partial transmit sequences," *IEEE Commun. Lett.,* vol. 4, no. 3, pp. 86–88, Mar. 2000.

[29] A. Alavi, C. Tellambura, and I. Fair, "PAPR reduction of OFDM signals using partial transmit sequence: an optimal approach using sphere decoding," *IEEE Commun. Lett.,* vol. 9, no. 11, pp. 982–984, Nov. 2005.

[30] L. Wang and Y. Cao, "Sub-optimum PTS for PAPR reduction of OFDM signals," *Electron. Lett.,* vol.44, no. 15, pp. 921–922, Jul. 2008.

[31] Y.-J. Cho, J.-S. No, and D.-J. Shin "A new low-complexity PTS scheme based on successive local search using sequences," *IEEE Commun. Lett.,* vol. 16, no. 9, pp. 1470–1473, Sep. 2012.

[32] Y.-J. Cho, J.-S. No, and D.-J. Shin "PTS scheme with low complexity for PAPR reduction by using Kasami sequences," *in Proc. KICS Int. Conf. Commun.,* pp. 120, May 2011.

[33] T. T. Nguyen and L. Lampe, "On partial transmit sequences for PAR reduction in OFDM system," *IEEE Trans. Wirelss Commun.,* vol. 7, no. 2, pp. 746–755, Feb. 2008.

[34] J. -H. Wen, S. -H. Lee, and Y.-F. Hunag, "A suboptimal PTS algorithm based on particle swarm optimization for PAPR reduction in OFDM systems," *EURASIP J. Wireless Commun. Netw.,* vol. 2008, article no. 14.

[35] Y. Zhang, Q. Ni, and H. -H. Chen, "A new partial transmit sequence scheme using genetic algorithm for peak-to-average power ratio reductionin a multi-carrier code division multiple access wireless system," *Interantional J. Autonomous Adaptive Commum. Systems,* vol. 2, no. 1/2009, pp. 40–57.

[36] N. Taspinar, A. Kalinli, and M. Yildirim, "Partial transmit sequences for PAPR reduction using parallel tabu search algorithm in OFDM systems," *IEEE Commun. Lett.,* vol. 15, no. 9, pp. 974–976, Sep. 2011.

[37] Y. Wang, W. Chen, and C. Tellambura, "A PAPR reduction method based on artificial bee colony algorithm for OFDM signals," *IEEE Trans. Wirelss Commun.*, vol. 9, no. 10, pp. 2994–2999, Oct. 2010.

[38] S. -J. Ku, C. -L. Wang, and C. -H. Chen, "A reduced-complexity PTS-based PAPR reduction scheme for OFDM systems," *IEEE Trans. Wirelss Commun.,* vol. 9, no. 8, pp. 2455–2460, Aug. 2010.

[39] Y. Xiao, X. Lei, Q. Wen, and S. Li, "A class of low complexity PTS techniques for PAPR reduction in OFDM systems," *IEEE Sinal Process. Lett.,* vol. 14, no. 10, pp. 680–683, Oct. 2007.

[40] Y.-J. Cho, J.-S. No, and D.-J. Shin, "Low-complexity PTS scheme for reducing PAPR in OFDM systems," *J. Commun. Netw.,* vol. 38A, no. 2, pp. 201–208, Feb. 2013.

[41] T. Kasami, "Weight distribution formula for some class of cyclic codes," Tech. Report No. R–285, Univ. of Illinois, 1966.

[42] P. V. Kumar, T. Helleseth, A. R. Calderbank, and A. R. Hammons, Jr, "Large families of quaternary sequences with low correlation," *IEEE Trans. Inf. theory.,* vol. 42, no. 2, pp. 579–592, Mar. 1996.

[43] T. H. Cormen, C. E. Leiserson, R. L. Rivest, and C. Stein, *Introduction to Algorithms,* 3rd ed. Cambridge, MA: MIT Press, 2009.

초 록

본 논문은 직교주파수분할다중화 시스템의 최대전력대평균전력비를 감소시키는 몇가지 방법을 제안한다. 먼저 직교주파수분할다중화 시스템의 기본원리, 최대전력대평균전력비의 정의, 비선형고출력증폭기를 설명한다. 직교주파수분할다중화 시스템에서 최대전력대평균전력비는 가장 큰 단점중의 하나이며 이는 비선형고출력증폭기에서 신호의 왜곡을 발생시키는 원인이 된다. 많은 최대전력대평균전력비의 감소 방법이 제안되어져 왔으며 그 중에 클리핑 기법, 선택사상기법, 부분전송수열, 능동형 심볼성상 확장기법, 압축확장기법, 톤삽입 기법등이 있다. 그중에 부분전송 수열은 많은 후보신호를 생성한 후에 가장 작은 최대전력대평균전력비를 가지는 신호 하나를 선택하여 전송하는 기법이다. 그러나 이 부분전송 수열은 몇번의 역퓨리에변환과 많은 후보신호의 생성이라는 계산복잡도를 가지고 있다. 우리는 여기서 후자의 계산복잡도를 감소시키는데 집중한다.

논문의 첫번째 분야에서는 새로운 저복잡도를 가지는 부분 전송 수열 기법이 제안되어지는데 여기서는 좋은 최대전력대평균전력비를 가지는 위상벡터들을 찾는 것을 두가지 연속적인 단계로서 제안한다. 첫번째 단계는 초기 위상 벡터라고 불리는데 상호연관성이 매우 낮은 수열을 이용하여 이를 위상 벡터로서 사용한다. 여기서는 카사미 수열과 4진 수열이 사용되어진다. 두번째 단계에서는 지역적인 탐색을 수행하는데 이는 먼저 초기 위상 벡터에 기본을 두고 좋은 최대전력대평균전력비를 가지는 추가적인 위상 벡터를 찾는 것을 말한다. 수적 분석은 제안하는 방법이 기존의 방법이나 기존에 제안된 저복잡도 부분 전송 수열 방법보다 훨씬

적은 계산복잡도로 좋은 성능을 보여준다.

논문의 두번째 분야에서는 또다른 저복잡도 부분 전송 수열 방법이 제안되어진다. 이때는 후보신호를 만들기 위한 덧셈과 곱셈을 줄이는데 집중한다. 우선적인 샘플이 선택되어지는데 이러한 샘플들은 후보신호의 최대전력대평균전력비를 계산하기 위해서 위상 벡터와 곱해진다. 제안하는 방법은 이러한 우선적인 샘플을 찾기위한 미터법을 생성한다. 이를 위해 세가지의 미터법이 제안되어진다. 또한 더 많은 계산복잡도를 감소시키기 위해 선택된 우선적인 샘플들은 미터법의 크기에 따른 순서대로 재배열되고 각각의 파워들은 전 후보신호의 최대전력대평균전력비와 비교되어진다. 또한 위상 벡터의 갯수도 미터법을 관찰함으로서 미리 제거되어진다. 수적 분석은 이러한 방법이 어떠한 최대전력대평균전력비의 손실도 없이 다른 저복잡도 부분 전송 수열 방법보다 더 낮은 계산복잡도를 가진다는 것을 볼 수 있다.

논문의 마지막 분야에서는 우선적인 샘플을 선택하기 위한 새로운 선택 방법이 제안되어지는데 이때 신호 공간에서 첫번째 서브블록의 샘플이 위치해있는 그 지역으로 모든 시간축 신호들을 돌려준다. 더구나 위상 벡터의 우선 제거 방법이 후보 신호의 개수를 줄이기 위해 제안되어진다. 따라서 세가지의 제안하는 부분 전송 수열 기법이 제안되어지는데 이는 단순한 신호 회전과 위상벡터의 우선 제거 방법을 이용한다. 후보신호의 최대전력대평균전력비를 계산하기 위한 복잡도는 새로운 간단한 제안하는 미터법을 이용한 우선 신호의 선택에 의해서 감소되어진다. 또한 위상 벡터의 우선 제거방법에 의해 후보신호의 개수가 제거되어진다. 수적 분석은 제안하는 부분 전송 수열 기법들이 기존 방법과 같은 최대전력대평균전력비를 가지면서 계산복잡도는 크게 감소한다.

주요어: 부분전송수열, 역퓨리에 변환, 위상 회전 벡터, 직교주파수분할 다중화, 최대전력대평균전력비, 카사미 수열, 퓨리에 변환, 4진 수열.

학번: 2010-30801

감사의 글

이제 말로 표현할 수 없는 그분의 선물로 인하여 하나님께 감사를 드리노라 (고린도후서 9 : 15)

나를 향한 주의 모든 베푸심을 내가 주께 무엇으로 보답할까?
(시편 116 : 12)

하나님께서 세상을 이처럼 사랑하셔서 그의 독생자를 주셨으니, 이는 그를 믿는 사람은 누구든지 멸망하지 않고 영생을 얻게 하려 하심이니라 (요한복음 3 : 16)